Am J Transl Res 2022;14(6):3750-3768
www.ajtr.org /ISSN:1943-8141/AJTR0142565

Original Article

A systematic pan-cancer analysis identifies RIOK3 as an immunological and prognostic biomarker

Jian Li[1], Ruili Sun[2], Lixiang He[1], Guoyi Sui[1], Wenyu Di[1], Jian Yu[1], Wei Su[1], Zenggang Pan[3], Yu Zhang[4], Jinghang Zhang[1], Feng Ren[1,4,5]

[1]Department of Pathology, The First Affiliated Hospital of Xinxiang Medical University, Xinxiang 453003, Henan, China; [2]Henan Key Laboratory of Immunology and Targeted Drugs, School of Laboratory Medicine, Xinxiang Medical University, Xinxiang 453003, Henan, China; [3]Department of Pathology, Yale University School of Medicine, New Haven, CT 06520, US; [4]School of Basic Medical Sciences, Xinxiang Medical University, Xinxiang 453003, Henan, China; [5]Henan International Joint Laboratory of Immunity and Targeted Therapy for liver-Intestinal Tumors, Xinxiang 453003, Henan, China

Received February 26, 2022; Accepted May 11, 2022; Epub June 15, 2022; Published June 30, 2022

Abstract: Objectives: Despite recent research highlighting the critical function of RIO kinase 3 (RIOK3) in a variety of malignancies, a comprehensive evaluation of RIOK3 in human tumors is absent. Our study helps to clarify the molecular mechanism of RIOK3 in carcinogenesis from multiple perspectives. Methods: Our research looked into the potential oncogenic role of RIOK3 in 33 cancers using TCGA (The Cancer Genome Atlas), GTEx (Genotype-Tissue Expression Project), GEO (Gene Expression Omnibus) datasets, and several bioinformatics tools. Results: RIOK3 expression in tumors is disordered compared to normal tissue, and it is highly linked with the level of MMR (Mismatch repair) gene mutations and DNA methyltransferase expression. According to univariate survival analysis, it could be used as an independent prognostic factor. Further investigation demonstrated that RIOK3 expression was correlated with cancer-associated fibroblast, neutrophil, and endothelial infiltration levels in kidney cancer and was positively correlated with the expression of immune checkpoint markers in different cancers. The functional pathways of RIOK3 also included cell-cell adhesion, protein phosphorylation, and innate immune-related functions. Conclusions: These findings suggest that RIOK3 could be used as an immunological and prognostic biomarker in various malignant tumors.

Keywords: RIOK 3, pan-cancer, prognosis, immune infiltration, methylation

Introduction

Cancer is caused by genetic variation, and the advent of massive parallel sequencing has made it possible to document this variation at the whole-genome level [1-3]. A large number of tumor-related functional genomic datasets have been used for exome, transcriptome, and DNA methylome data analysis to draw a comprehensive picture of commonalities, differences, and emerging themes among tumor types using publicly funded cancer genomics databases and repositories, such as The Cancer Genome Atlas (TCGA) and Gene Expression Omnibus (GEO) [4-7]. Pan-cancer studies have been widely used to investigate the common characteristics or heterogeneities involved in the occurrence and progression of tumors [5, 8]. Pathway genes have also been identified using pan-cancer research, allowing for the collection of a broad range of in-depth information on the molecular mechanisms connected to malignancy [9-11]. Given the intricacy of carcinogenesis, conducting a pan-cancer expression analysis of any gene of interest and assessing its link with clinical prognostic value and potential molecular pathways is critical.

RIOK1, RIOK2, and RIOK3 are right open reading frame (RIO) kinases. RIOK1 and RIOK2 are found from archaea to humans, whereas RIOK3 is exclusively found in multi-cellular eukaryotes [12]. RIOK3 knockdown increases the amount of 21S pre-rRNA in the 18S rRNA synthesis pathway in human cells [13]. The development of the 40S ribosomal subunit is dependent on

this pre-rRNA processing [14]. These findings suggest that RIO kinases play an important role in ribosome biosynthesis in mammalian cells. Recent studies have discovered that RIOK3 is essential for actin cytoskeletal organization [15], that knocking down RIOK3 slows cell migration and invasion in breast and pancreatic cancer cells [15, 16], and that high RIOK3 levels in gliomas appear to contribute to the tumor's development and expansion [17]. Furthermore, RIOK3 expression is elevated in metastatic head and neck cancers [18], while RIOK3 expression in malignant melanomas was significantly lower at the invasive front than in the tumor center [19]. The previously established role of RIOK3 in ribosomal biosynthesis regulation and its role in tumor growth and metastasis suggest the hypothesis that RIOK3 plays a vital role in cancer genesis and progression. However, earlier research limited the evaluation of RIOK3 to a few tumor types, and its functions in additional tumor types remained unknown.

We used previously described methodologies [20] to systematically characterize the functions and prognostic value of RIOK3 in various cancers in this investigation. We used information from the TCGA Project and the GEO databases to investigate the expression profile of RIOK3 across diverse tumor types in a pan-cancer analysis. To investigate the potential molecular mechanism of RIOK3 in the pathogenesis or clinical prognosis of multiple tumors, we looked at many factors, including survival status, genetic alterations, DNA methylation, immune infiltration, and tumor mutational burden (TMB), microsatellite instability (MSI), and relevant cellular pathways.

Materials and methods

Gene expression analysis

GEPIA2 (Gene Expression Profiling Interactive Analysis, version 2, http://gepia2.cancer-pku.cn/) [21] has been a valuable and highly cited resource for gene expression analysis on tumor and normal samples from the TCGA and the GTEx (Genetype-Tissue Expression Project) databases. It was utilized to compare the expression of RIOK3 in tumors and normal tissues from various cancers or tumor subtypes in the TCGA project. The GEPIA2 tool was also utilized to examine RIOK3 expression in all TCGA tumors at various pathological stages. For the dot and violin plots, log2 [TPM (Transcripts per million) +1] converted expression data were used.

The UALCAN portal (http://ualcan.path.uab.edu/analysis-prot.html) [22], an interactive web resource for analyzing cancer Omics data, was used to analyze protein expression from the Clinical proteomic tumor analysis consortium (CPTAC) dataset. The expression of the RIOK3 protein has been compared between primary tumors and normal tissues.

Survival prognosis analysis

Overall survival (OS) and disease-free survival (DFS) significance map data and survival plots of RIOK3 across all TCGA cancers were also obtained using GEPIA2. In this analysis, the group cutoff values of the high-expression and low-expression groups were set to 50%. The Kaplan-Meier Plotter (http://kmplot.com/analys is/) [23] is a meta-analysis tool for discovering and validating survival biomarkers. The system, including datasets from GEO, The European Genome-phenome Archive (EGA), and TCGA, can assess the survival value of 54,000 genes across 21 cancer types. In this study, the group cutoff values of the high-expression and low-expression groups were set to the best cutoff. Hazard ratios with 95% confidence intervals and log-rank *P* values were also calculated.

Genetic alteration analysis

cBioPortal (http://cbioportal.org) [24, 25] is an open resource for interactive exploration of multiple sets of cancer genomics data. It was utilized to gather data on RIOK3 alteration frequency, mutation type, altered site information, and copy number alteration (CNA) across all TCGA tumors in this study. All TCGA cancer types, with or without RIOK3 genetic changes, had their survival data compared, including overall survival (OS), progression-free survival (PFS), disease-specific survival (DSS), and disease-free survival (DFS).

ESTIMATEScore was estimated using the Sangerbox tool platform (http://www.sangerbox.com/tool) to investigate the correlation between RIOK3 expression and TMB and MSI in all TCGA tumors. On the Sangerbox tool platform, a related technique is based on an R

script for the ESTIMATE algorithm, which may also be done with R software.

The TCGA database was applied to determine five mismatch repair (MMR) gene mutation levels (MLH1, MSH2, MSH6, PMS2, and EPCAM). The link between RIOK3 expression and MMR gene mutation levels was investigated using Pearson correlation analysis.

DNA methylation analysis

The SMART App (http://www.bioinfo-zs.com/smartapp) [26] was applied to investigate methylation value and the correlation between gene expression and methylation values in different tumors based on the TCGA project. The relationship between the expression level of RIOK3 and that of 4 methyltransferases (DNMT1, DNMT2, DNMT3A, and DNMT3B) was evaluated by Pearson correlation analysis. The DNMIVD tool [27] was used to perform the survival analyses between the methylation value of RIOK3 and the prognosis in different cancer patients in the TCGA database.

Immune infiltration analysis

Tumor immune estimation resource, version 2.0 (TIMER2.0, http:// timer.cistrome.org/) [28] was used to analyze the relationship between RIOK3 expression and immune infiltration across all TCGA tumors. The TIMER, TIDE, CIBERSORT, CIBERSORT-ABS, QUANTISEQ, XCELL, MCPCOUNTER, and EPIC algorithms were applied for estimations. The TIMER database was used to obtain the scores of invading immune cells in 33 malignancies. The connection between RIOK3 expression and immunological infiltration and immune checkpoint marker expression levels were assessed using Pearson correlation analysis. Gene expressions are shown as log2 (TPM+1) values.

Gene enrichment analysis

STRING v11 (https://string-db.org/) [29] was used for the subsequent analysis of the protein-protein interaction network. The main parameter settings were as follows: the meaning of network edges = “evidence”, active interaction source = “Textmining” and “Experiments”, minimum required interaction score = “Low confidence (0.150)”, max number of interactors to show = “no more than 50 interactors” in the 1st shell. Based on the datasets of all TCGA tumors and normal tissues, GEPIA2 was used to find the top 100 RIOK3-correlated genes. The two datasets were then integrated to perform the KEGG pathway and Gene Ontology (GO) enrichment analysis using the web-based application DAVID 6.8 (https://david. ncifcrf.gov) [30]. The results were visualized in a Bar plot using ggplot2 in the R software (V 4.0.1, 64-bit) environment.

Statistical methods

T-tests were used to estimate changes in expression levels and methylation values in cancer and normal tissues. The HR and *P*-value for survival analysis were calculated using univariate Cox regression analysis. Furthermore, Pearson or Spearman correlation was applied to analyze the correlation among different gene expressions. Above all, $P < 0.05$ was set as statistically significant if there was no special annotation.

Results

Pan-cancer expression landscape of RIOK3

The conservation of RIOK3 among different species was investigated to offer a complete analysis of the role of human RIOK3 (NM 003831.5 for mRNA or NP 003822.2 for protein, Figure S1A). RIOK3 protein structure is conserved across species (e.g., Homo sapiens, Mus musculus, Rattus norvegicus) and usually comprises a Catalytic (cd05146) domain (Figure S1B). The significant conservation of RIOK3 suggests that it may be involved in basic biological processes.

RIOK3 has the highest expression in bone marrow, followed by the esophagus, skeletal muscle, and small intestine, according to a combination of the human protein atlas (HPA), GTEx, and function annotation of the mammalian genome 5 (FANTOM5) datasets (Figure S2A). RIOK3 was ubiquitously expressed in almost all tissues (all consensus normalized expression values > 1), with limited tissue specificity in its mRNA expression. When HPA/Monaco/Schmiedel datasets were analyzed, basophils had the greatest RIOK3 expression, followed by nonclassical monocytes and intermediate monocytes (Figure S2B). Low RNA blood cell-type specificity was also discovered.

Then, using tumor and normal samples from the TCGA and GTEx databases, GEPIA2 was utilized to analyze gene expression. According to the findings, RIOK3 mRNA expression was uneven among the TCGA tumor types. In ACC (Adrenocortical carcinoma), BLCA (Bladder urothelial carcinoma), BRCA (Breast invasive carcinoma), CHOL (Cholangiocarcinoma), COAD (Colon adenocarcinoma), ESCA (Esophageal carcinoma), KICH (Kidney chromophobe), LAML (Acute myeloid leukemia), LUAD (Lung adenocarcinoma), OV (Ovarian serous cystadenocarcinoma), PRAD (Prostate adenocarcinoma), READ (Rectum adenocarcinoma), SKCM (Skin cutaneous melanoma), TGCT (Testicular germ cell tumors), THCA (Thyroid carcinoma), UCEC (Uterine corpus endometrial carcinoma), and UCS (Uterine carcinosarcoma), the expression level of RIOK3 was significantly lower than that in adjacent normal tissues (**Figure 1A**, $P < 0.05$). In contrast, RIOK3 showed higher expression in GBM (Glioblastoma multiforme), KIRC (Kidney renal clear cell carcinoma), KIRP (Kidney renal papillary cell carcinoma), LGG (Brain lower-grade glioma), PAAD (Pancreatic adenocarcinoma), and STAD (Stomach adenocarcinoma) (**Figure 1A**, $P < 0.05$). Meanwhile, a significant difference for other tumors was not obtained, such as CESC (Cervical squamous cell carcinoma and endocervical adenocarcinoma), DLBC (Lymphoid neoplasm diffuse large B-cell lymphoma), HNSC (Head and neck squamous cell carcinoma), and LIHC (Liver hepatocellular carcinoma) (**Figure 1A**, $P > 0.05$).

Further analysis of RIOK3 protein expression using the CPTAC database revealed that in BRCA ($P < 0.05$), KIRC ($P < 0.0001$), UCEC ($P < 0.01$), and LUAD ($P < 0.01$), RIOK3 protein expression was considerably higher in tumor tissues compared to normal tissues, but it was decreased in COAD ($P < 0.001$) (**Figure 1B**). The RIOK3 mRNA does not match the protein expression, indicating that it is sensitive to post-transcriptional regulation by various factors.

Pan-cancer analysis of the multifaceted prognostic value of RIOK3

The researchers investigated the relationship between RIOK3 expression and prognosis in patients with various malignancies, utilizing the TCGA and GEO datasets. Tumor cases in the TCGA were classified into high-expression and low-expression groups based on RIOK3 expression levels. For the TCGA instances of ACC ($P = 0.031$), LGG ($P = 0.00016$), PAAD ($P = 0.031$), and PRAD ($P = 0.0062$), OS analysis results (**Figure 2A**) revealed a link between high RIOK3 expression and poor prognosis. Highly expressed RIOK3 was linked to a poor prognosis of DFS for cancers of ACC ($P < 0.0001$) and LGG ($P = 0.0066$) within the TCGA project (**Figure 2B**). Furthermore, decreased RIOK3 expression was linked to a poor OS and DFS prognosis for KIRC patients (**Figure 2A** and **2B**, $P < 0.0001$ and $P = 0.0012$).

Survival data was also analyzed by the Kaplan Meier plotter (database sources include GEO, EGA, and TCGA) tool. It was found that there was a correlation between high RIOK3 expression level and better prognosis of OS ($P = 0.012$), first progression (FP) ($P = 0.027$) and post-progression survival (PPS) ($P < 0.0001$) in gastric cancer (Figure S3A). In lung cancer, high RIOK3 expression level was related with poor OS ($P = 0.0034$), better FP ($P = 0.042$), and PPS ($P = 0.0012$) (Figure S3B). In ovarian cancer, high levels of RIOK3 were positively correlated with OS ($P = 0.05$), but there was no significant statistical significance for PFS and PPS (Figure S3C). For breast cancer patients with high level of RIOK3 expression, the prognosis of distant metastasis-free survival (DMFS) ($P = 0.0017$), PPS ($P < 0.0001$) and PFS were poor ($P = 0.034$) (Figure S3D). In addition, for patients with liver cancer, the expression of RIOK3 had no significant correlation with their prognosis (Figure S3E). These findings suggest that RIOK3 is critical in cancer prognosis.

Low RIOK3 mRNA expression is also substantially associated with advanced tumor stages, such as ESCA ($P = 0.0165$) and LIHC ($P = 0.00946$), according to stage maps in the GEPIA database. PAAD also had a stage-specific expressional change in RIOK3 ($P = 0.0416$) (**Figure 2C**). While, in most tumors, no clear association was found (Figure S4).

Pan-cancer analysis of the genetic alteration of RIOK3

The pan-cancer alteration of RIOK3 was investigated using the cBioPortal database. The frequency of RIOK3 alteration (> 12%) was the highest in PAAD, with *amplification* as the primary type. UCEC had the highest incidence of

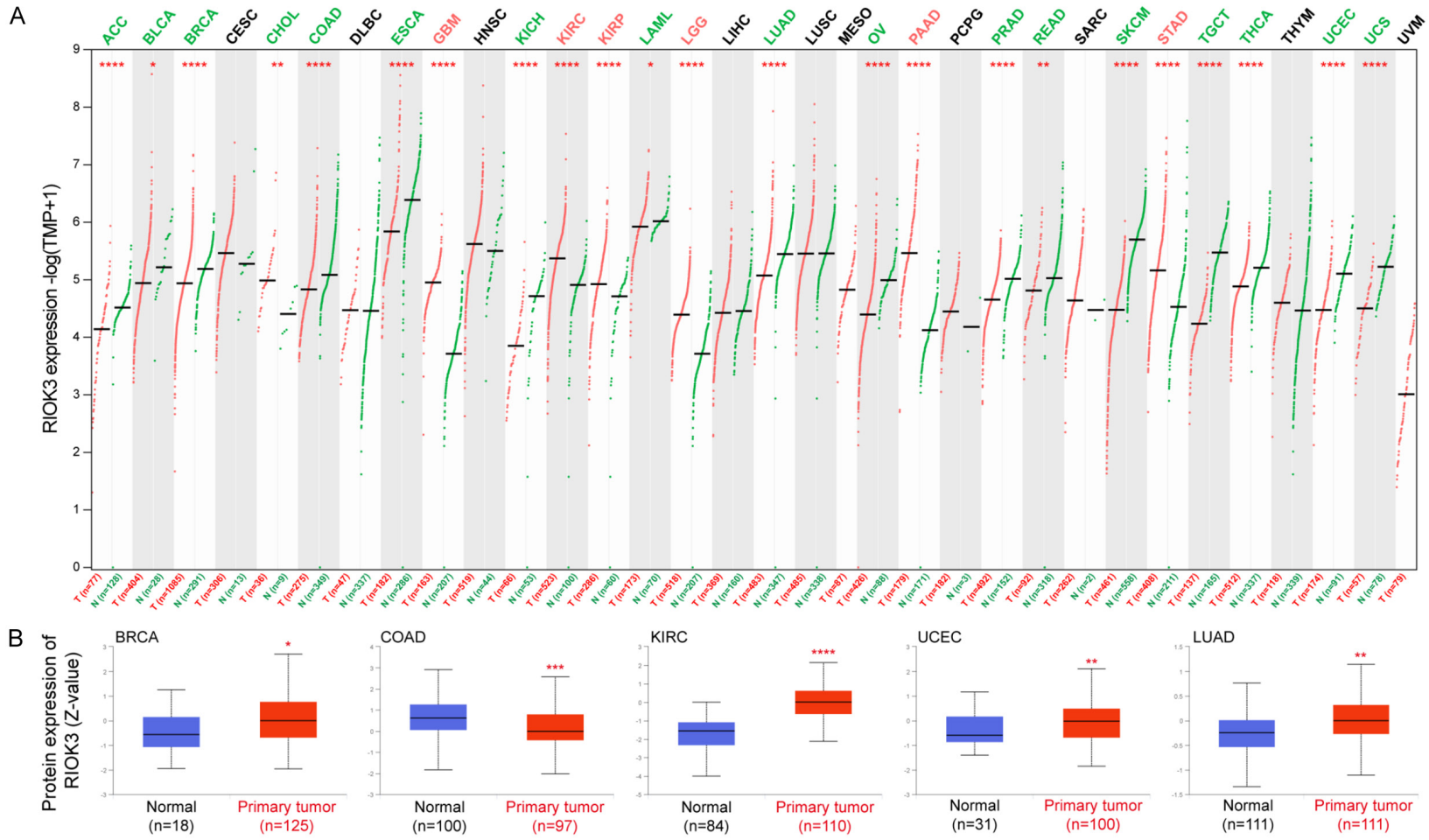

Figure 1. RIOK3 expression levels in different tumors. A. Expression levels of RIOK3 in different tumors were analyzed by GEPIA2. B. Expression levels of RIOK3 total protein in BRCA, COAD, KIRC, UCEC, and LUAD were analyzed by CPTAC. *P < 0.05; **P < 0.01; ***P < 0.001; ****P < 0.0001.

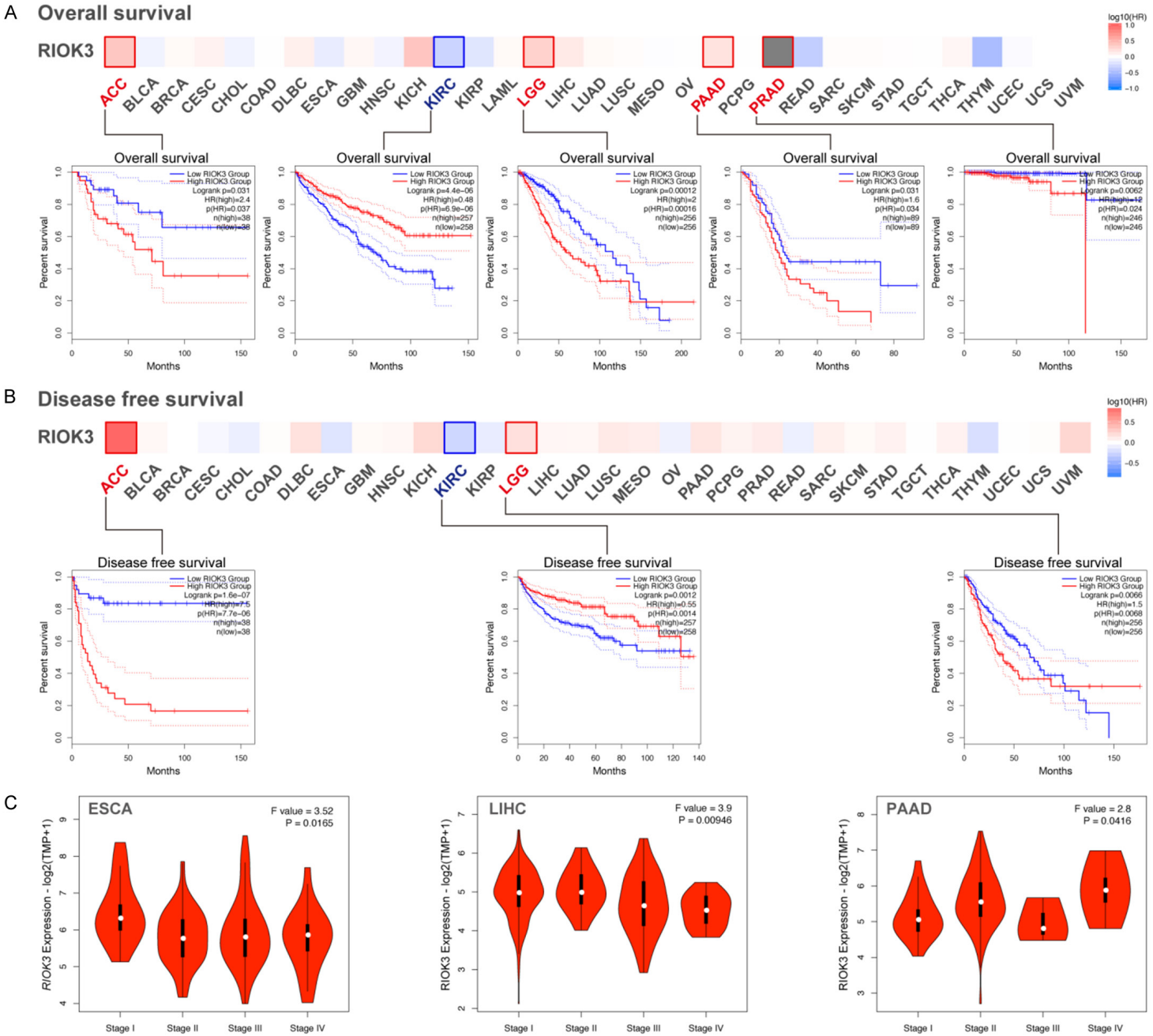
A
Overall survival
RIOK3
log10(HR)
ACC BLCA BRCA CESC CHOL COAD DLBC ESCA GBM HNSC KICH KIRC KIRP LAML LGG LIHC LUAD LUSC MESO OV PAAD PCPG PRAD READ SARC SKCM STAD TGCT THCA THYM UCEC UCS UVM
Overall survival
Low RIOK3 Group
High RIOK3 Group
Percent survival
Months
B
Disease free survival
RIOK3
log10(HR)
ACC BLCA BRCA CESC CHOL COAD DLBC ESCA GBM HNSC KICH KIRC KIRP LGG LIHC LUAD LUSC MESO OV PAAD PCPG PRAD READ SARC SKCM STAD TGCT THCA THYM UCEC UCS UVM
Disease free survival
Low RIOK3 Group
High RIOK3 Group
Percent survival
Months
C
ESCA
F value = 3.52
P = 0.0165
LIHC
F value = 3.9
P = 0.00946
PAAD
F value = 2.8
P = 0.0416
RIOK3 Expression - log2(TMP+1)
Stage I
Stage II
Stage III
Stage IV

Figure 2. Correlation between RIOK3 expression and prognosis of tumors in TCGA. A and B. Relationship between RIOK3 expression and overall survival and disease-free survival were assessed in all TCGA tumors using GEPIA2. The survival map and Kaplan-Meier curves with positive results (P < 0.05) are given. C. The stage-dependent expression level of RIOK3. Main pathological stages (stage I, stage II, stage III, and stage IV) of ESCA, LIHC, and PAAD were assessed and compared using TCGA data.

mutation, with a frequency of > 4% (**Figure 3A**). It is worth noting that all uterine mixed endometrial carcinoma (the subtype of UCEC) cases with RIOK3 alteration had a mutation (~5% frequency) (**Figure 3B**). All MESO (Pleural mesothelioma) cases with RIOK3 genetic alteration (> 2% frequency) had *structural variants,* and all TGCT cases had copy number *deep deletion* (~2% frequency) (**Figure 3A**). The types, sizes, and numbers of RIOK3 genetic mutations are investigated further, revealing that missense mutations were the most common type of RIOK3 mutation (**Figure 3C**). In addition, the potential link between RIOK3 genetic alterations and clinical survival prognosis was investigated in a variety of malignancies, with only UCEC showing a meaningful correlation. Compared with cases without RIOK3 mutation, UCEC cases with RIOK3 mutation appeared better prognosis in OV (P = 0.0354) and PFS (P = 0.0498), but no clear correlation with DSS (P = 0.0669) and DFS (P = 0.330) (**Figure 3D**).

The relationships between RIOK3 expression and TMB and MSI were explored across all tumors in TCGA. The results showed that the expression level of RIOK3 was positively correlated with TMB in ACC (P = 0.00043), GBM (P = 0.049), ESCA (P = 0.032), PAAD (P = 0.00028), SARC (Sarcoma) (P = 0.027), COAD (P = 1.3e-07), STAD (P = 1.4e-05), SKCM (P = 0.00096), and LGG (P = 1.9e-05), but negatively correlated with THCA (P = 0.0075) (**Figure 4A**). The RIOK3 expression level was also positively correlated with MSI in UCEC (P = 0.00033), COAD (P = 4.4e-09), STAD (*P* = 1.4e-05), and READ (P = 3e-05), but negatively correlated with DLBC (P = 0.013), LUAD (P = 0.0042), PRAD (P = 7.7e-05), SKCM (P = 0.016), and HNSC (P = 0.019) (**Figure 4B**). The relationship between RIOK3 expression and the levels of mismatch repair (MMR) gene mutations was also investigated. In almost all TCGA cancers, RIOK3 expression was positively linked with mutation levels of five MMR genes (MLH1, MSH2, MSH6, PMS2, and EPCAM) (**Figure 4C**). These results suggest that RIOK3 may mediate TMB and MSI through influencing the MMR system, thus promoting tumor genesis and development.

Pan-cancer methylation analysis of RIOK3

Using the SMART methods based on the TCGA database, the DNA methylation of RIOK3 was studied, and a substantial decrease in the promoter methylation level of RIOK3 was identified in BLCA (P < 0.0001), BRCA (P < 0.01), CESC (P < 0.05), HNSC (P < 0.05), KIRP (P < 0.0001), LUAD (P < 0.0001), LUSC (P < 0.0001), READ (P < 0.05), THCA (P < 0.0001), and UCEC (P < 0.05) tissues, but a signicant increase in KIRC (P < 0.05), compared to normal tissues (**Figure 5A**). In addition, the correlation between RIOK3 expression and DNA methyltransferase (DNMT, including DNMT1, DNMT2, DNMT3, and DNMT4) expression was also analyzed. In most TCGA tumor types (21/33), a positive correlation was found between RIOK3 and DNMT (R > 0.2 and P < 0.05). Especially in ACC, BRCA, DLBC, KICH, KIRC, LGG, LIHC, PCPG, PRAD, SARC, SKCM, TGCT, THCA, THYM (Thymoma), and UVM (Uveal Melanoma), this correlation is more significant (R > 0.4 and P < 0.05) (**Figure 5B**). Furthermore, Pearson's correlation between methylation of RIOK3 promoter and RIOK3 expression was calculated. A significant negative correlation was found in CESC, CHOL, DLBC, ESCA, HNSC, LIHC, LUSC, PAAD, and STAD, and a significant positive correlation was observed in KICH, KIRC, TGCT, and UVM (|R| > 0.2 and P < 0.05) (**Figure 5C**). Furthermore, no significant correlation was found for other tumors, such as ACC, BLCA, BRCA, COAD, or GBM (|R| < 0.2 or P > 0.05) (Figure S5A).

The DNMIVD tool was also used to investigate a possible link between the methylation value of RIOK3 and clinical survival prognosis (Table S1). The results were as follows: the methylation level of RIOK3 was negatively correlated with the OV rate of ESCA (P = 0.041) and KIRC (P = 0.028) patients but positively correlated with the OV rate of LIHC (P = 0.027) patients (Figure S5B-D); For LIHC patients, the methylation level of RIOK3 is positively correlated with progression-free interval (PFI) (Figure S5E, P = 0.05); For PRAD patients, the methylation level of RIOK3 is negatively correlated with disease-free interval (DFI) and PFI (Figure S5F and S5G,

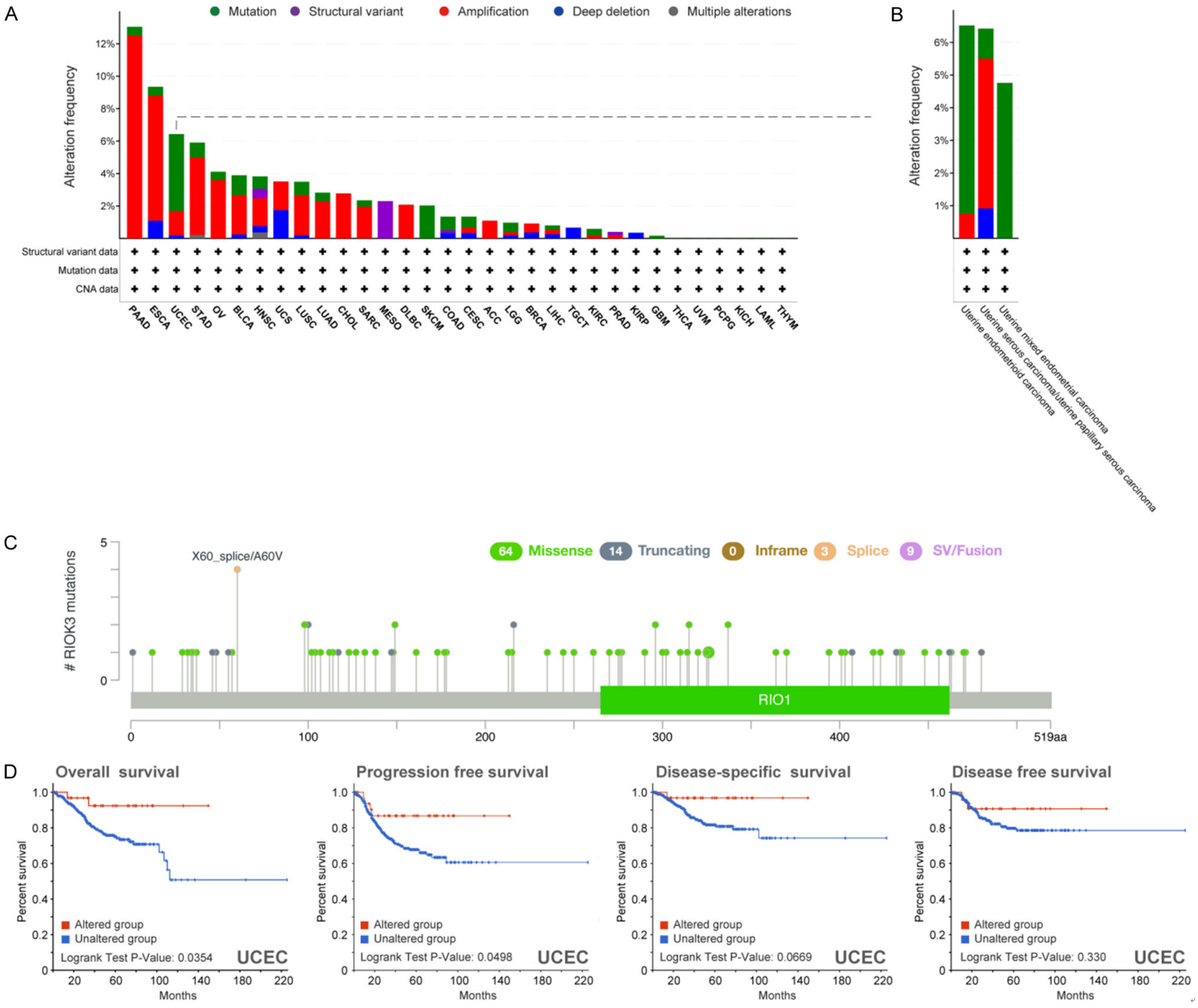
A
Mutation
Structural variant
Amplification
Deep deletion
Multiple alterations
Alteration frequency
12%
10%
8%
6%
4%
2%
Structural variant data
Mutation data
CNA data
PAAD ESCA UCEC STAD OV BLCA HNSC UCS LUSC LUAD CHOL SARC MESO DLBC SKCM COAD CESC ACC LGG BRCA LIHC TGCT KIRC PRAD KIRP GBM THCA UVM PCPG KICH LAML THYM
B
Alteration frequency
6%
5%
4%
3%
2%
1%
Uterine mixed endometrial carcinoma
Uterine serous carcinoma/uterine papillary serous carcinoma
Uterine endometrioid carcinoma
C
RIOK3 mutations
5
0
X60_splice/A60V
64 Missense
14 Truncating
0 Inframe
3 Splice
9 SV/Fusion
RIO1
0
100
200
300
400
519aa
D
Overall survival
Progression free survival
Disease-specific survival
Disease free survival
Percent survival
1.0
0.8
0.6
0.4
0.2
0
Altered group
Unaltered group
Logrank Test P-Value: 0.0354
Logrank Test P-Value: 0.0498
Logrank Test P-Value: 0.0669
Logrank Test P-Value: 0.330
UCEC
20 60 100 140 180 220
Months

Figure 3. Mutation feature of RIOK3 in TCGA tumors. A. The alteration frequency in different tumors of TCGA. B. The alteration frequency in subtypes of UCEC. C. The mutation sites in the RIOK3 gene. D. The correlation between mutation status and OS (overall survival), PFS (Progression-free survival), DSS (Disease-specific survival), and DFS (Disease-free survival) of UCEC. The above data are analyzed by the cBioPortal tool.

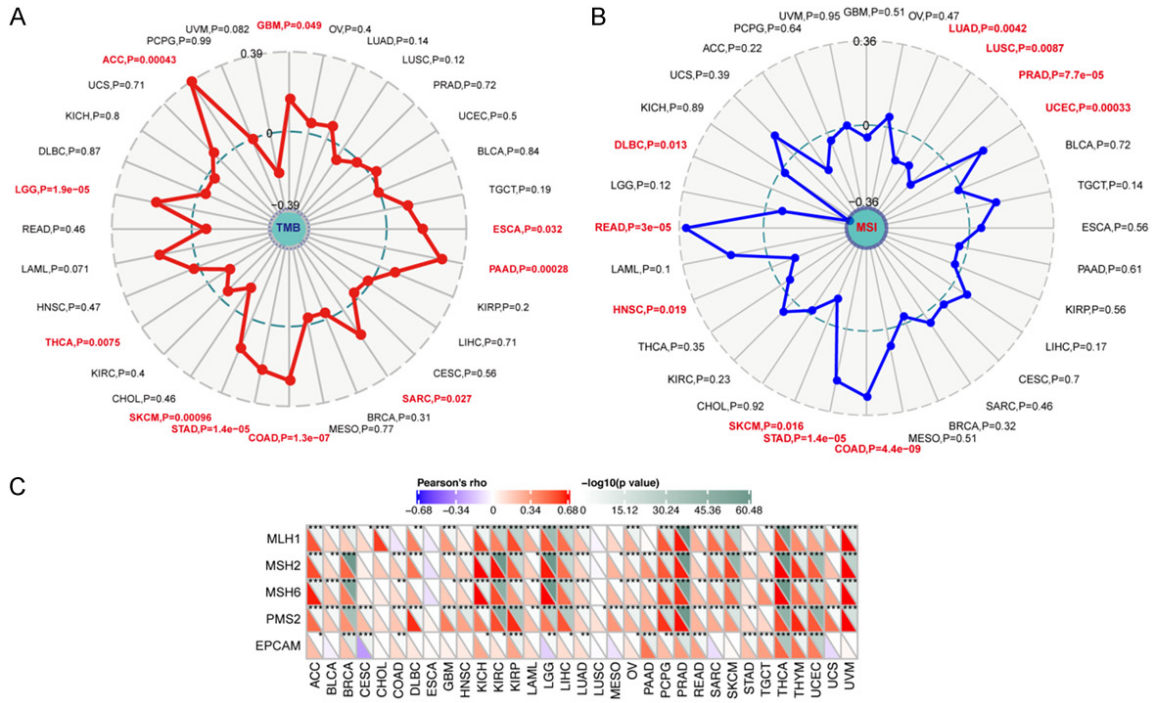

Figure 4. Correlation between RIOK3 expression and TMB and MSI. A. Correlation analysis of RIOK3 expression with TMB index based on TCGA data. The *P*-value and the partial correlation values of 0.39 and -0.39 are displayed. B. Correlation analysis of RIOK3 expression with MSI index based on TCGA database. The *P*-value and the partial correlation values of 0.36 and -0.36 are displayed. C. Correlation analysis of RIOK3 expression with the mutation levels of 5 MMR genes (MLH1, MSH2, MSH6, PMS2, and EPCAM) based on the TCGA database. (*P < 0.05; **P < 0.01; ***P < 0.001).

P = 0.05 and P = 0.0096). These data suggest that the expression of RIOK3 is regulated by promoter methylation, and RIOK3 is involved in the process of DNA methylation during tumor progression.

Pan-cancer analysis of the RIOK3 expression and immune cell infiltration

Considering the role of RIOK3 in the regulation of innate immune and actin cytoskeleton organization required for migration and invasion, we hypothesized that changes in RIOK3 expression or genetic changes could affect the tumor-infiltrating immune cell response [15, 17, 31]. Thus, the correlation between the infiltration degree of distinct immune or endothelial cells and RIOK3 expression was investigated in diverse tumor types of TCGA. The analysis results revealed that RIOK3 expression was adversely correlated with estimated infiltration values of cancer-associated fibroblasts in KIRC and STAD based on all algorithms (**Figure 6A**) but positively correlated with neutrophil cell infiltration in COAD and KIRC (**Figure 6B**). Moreover, RIOK3 expression and endothelial cell infiltration values for KIRC and TGCT showed a positive correlation (**Figure 6C**). Subsequently, the correlation between the expression of RIOK3 and 47 common immune checkpoint genes was investigated. It should be noted that in BRCA, COAD, KICH, KIRC, LGG, PRAD, READ, and UVM, RIOK3 expression is associated with more than 30 immune checkpoint markers, such as TNFRSF9, CD44, CD86, and CD274 (Figure S6). Altogether, these results strongly suggest that RIOK3 is important for tumor immunity.

A

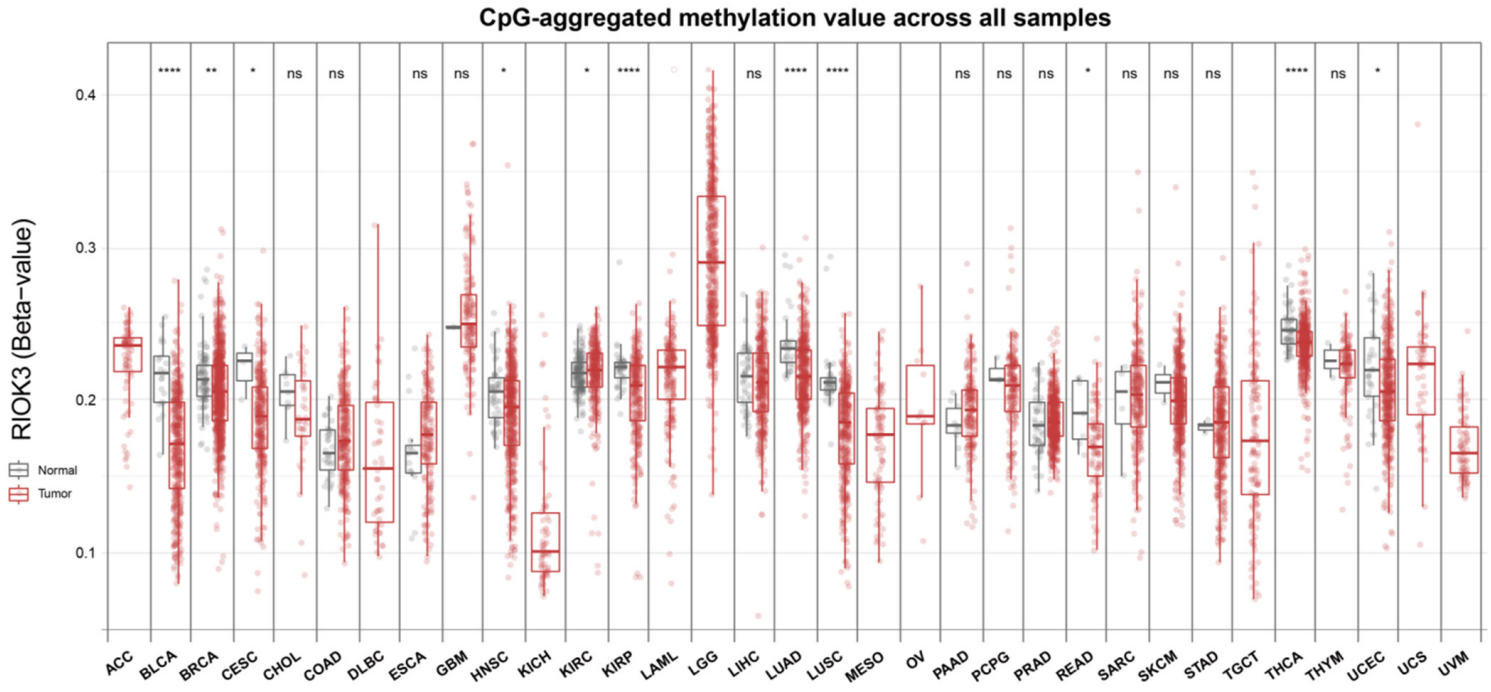
CpG-aggregated methylation value across all samples
RIOK3 (Beta−value)
0.4
0.3
0.2
0.1
Normal
Tumor
**** ** * ns ns ns ns * * **** ns **** **** ns ns ns * ns ns ns **** ns *
ACC BLCA BRCA CESC CHOL COAD DLBC ESCA GBM HNSC KICH KIRC KIRP LAML LGG LIHC LUAD LUSC MESO OV PAAD PCPG PRAD READ SARC SKCM STAD TGCT THCA THYM UCEC UCS UVM

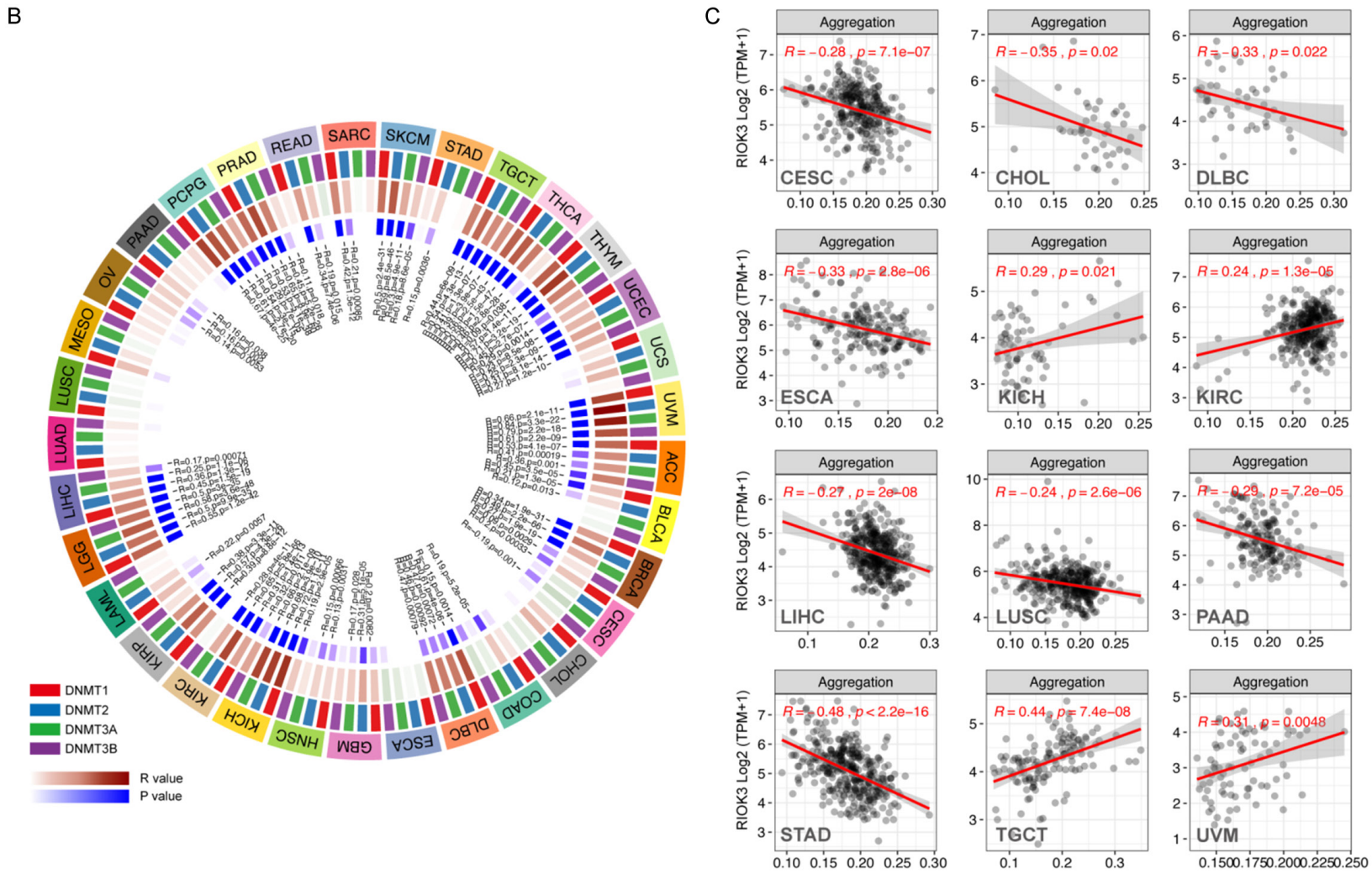

Figure 5. Analysis of RIOK3 DNA methylation data in TCGA. A. CpG-aggregated methylation value (beta-value) across all samples in TCGA project. *P < 0.05; **P < 0.01; ***P < 0.001; ****P < 0.0001. B. Correlation of RIOK3 expression with DNA methyltransferase (DNMT1, DNMT2, DNMT3, and DNMT4) expression. C. Correlation between gene expression and methylation value (beta-value) of RIOK3 in different tumors of TCGA. These data are statistically significant (R > 0.2 and P < 0.05).

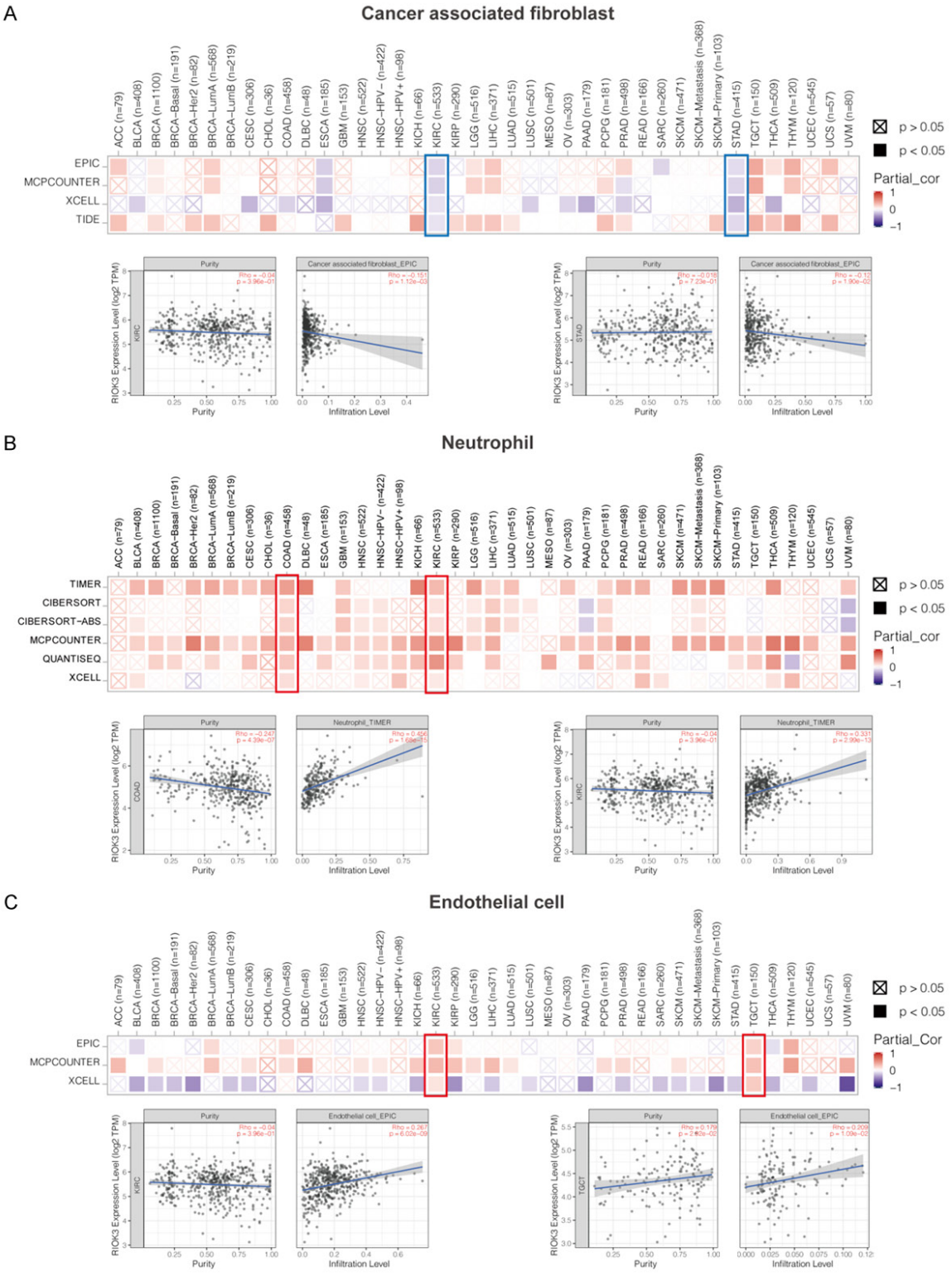

Figure 6. Analysis of the RIOK3 expression and immune cell infiltration. Correlation between RIOK3 expression level and infiltration of cancer-associated fibroblasts (A), neutrophils (B), and endothelial cells (C) across all tumors in TCGA. The red color indicates a positive correlation (0-1), while the blue represents a negative correlation (-1-0). The correlation with *P*-value < 0.05 is considered statistically significant. Statistically, non-significant correlations values are marked with a cross. Scatter plots with significant correlation are shown below.

Enrichment analysis of RIOK3-related partners

To further investigate the underlying mechanisms of the RIOK3 gene in tumorigenesis development, the RIOK3-binding proteins and RIOK3 expression-correlated genes were screened out in a series of pathway enrichment analyses. Based on the STRING database, 50 RIOK3-binding proteins were obtained (**Figure 7A**), supported by experimental evidence and text mining. Then, the GEPIA2 tool was used to obtain the top 100 genes that correlated with RIOK3 expression in all tumor types of TCGA. The RIOK3 expression was positively correlated with tropomodulin 3 (TMOD3) ($R = 0.53$), STE20 like kinase (SLK) ($R = 0.5$), kruppel like factor 3 (KLF3) ($R = 0.5$), protein kinase N2 (PKN2) ($R = 0.49$), mitogen-activated protein kinase 2 (MAP3K2) ($R = 0.48$), and other genes (all $P < 0.0001$) (Show only the top five, **Figure 7B** and **7C**).

Then, the above two data sets were combined for GO and KEGG enrichment analyses. The biological process (BP) of GO analysis suggested that RIOK3 might be related to cell-cell adhesion, protein phosphorylation, rRNA processing, peptidyl serine phosphorylation, positive regulation of I-kappaB kinase/NF-kappaB signaling, and others (**Figure 7D**, $P < 0.01$). The molecular function (MF) of GO analysis showed that protein binding, ATP binding, cadherin binding involved in cell-cell adhesion, protein serine/threonine kinase activity, and protein kinase activity might be affected by RIOK3 expression (**Figure 7E**, $P < 0.01$). The cellular component (CC) of GO analysis displayed multiple significant terms, such as cytoplasm, cytosol, nucleoplasm, cell-cell adherens junction, and others (**Figure 7F**, $P < 0.01$). The KEGG analysis identified several significant terms: endocytosis, salmonella infection, RIG-I-like receptor signaling pathway, adherens junction, and ribosome biogenesis of eukaryote (**Figure 7G**, $P < 0.05$).

Discussion

The multifunctional RIOK3 protein is involved in various pathological processes *in vivo*, including tumor etiology and progression. RIOK3 has been identified as a component of pre-40S preribosomal particles [13] and as a regulator of erythroblast enucleation [32]. By stimulating the AKT/mTOR signaling pathway in gliomas, RIOK3 increases tumor cell proliferation, motility, and invasion [17]. RIOK3 forms a complex with PAK1 in pancreatic cancer cells, which can alter the cytoskeleton structure and enhance cancer cell motility and invasion [16]. RIOK3 interacted with many proteins in breast cancer cells, including actin cytoskeleton components (ACTG1, ACTA2, TPM3, TPM4, and TMOD3) and ribosomal subunits (RPS3, RPS14, RPS16, RPS18, RPS20, RPL27A, RPL30) [15]. Other tumor-related and immune response signaling pathways that RIOK3 regulates include the Hedgehog and the NF-κB pathways [33, 34] because the wide range of subcellular protein interactions can play various regulatory roles in different systems and under different conditions.

The “HomoloGene” research data revealed that the RIOK3 protein structure is conserved across species, implying that similar processes may exist for RIOK3’s normal physiological role. Nonetheless, it is unclear whether RIOK3 is engaged in the oncogenesis of specific tumor types or plays a role in more common tumor pathogenesis pathways. As a result, we analyzed the RIOK3 gene in 33 distinct cancers using data from the TCGA, GTEx, CPTAC, and GEO databases and molecular parameters such as gene expression, genetic change, and DNA methylation.

Transcriptome analysis showed that the expression level of RIOK3 in most tumor tissues was lower than that in the corresponding normal tissues (17/33), and high expression was only observed in GBM, KIRC, KIRP, LGG, PAAD, and STAD tissues (6/33). In proteomic analysis, we found that the total protein expression levels of RIOK3 in BRCA, KIRC, UCEC, and LUAD were higher than that in their corresponding adjacent tissues, but the expression in COAD was decreased. Although we only obtained data on RIOK3 protein expression in 5 cancers, they were highly inconsistent with RIOK3 mRNA expression, indicating that some factors regulate RIOK3 after transcription. The most common examples are microRNA and methylation. Further analysis showed that the high expression level of RIOK3 was correlated with the poorer OV in ACC, LGG, PAAD, PRAD, and lung cancer, and better OV in KIRC, gastric cancer, and ovarian cancer compared with low expression level. In addition, in ESCA, LIHC, and

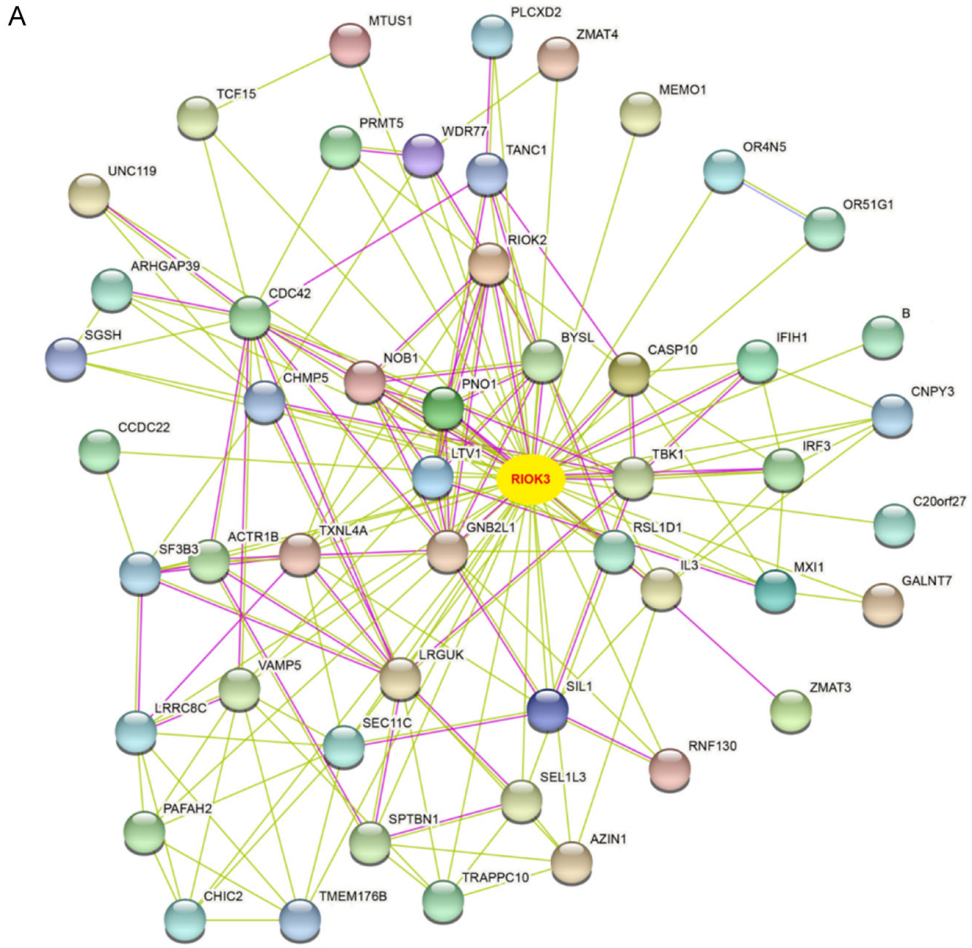
A
MTUS1
PLCXD2
ZMAT4
TCF15
MEMO1
PRMT5
WDR77
TANC1
OR4N5
UNC119
OR51G1
RIOK2
ARHGAP39
CDC42
SGSH
NOB1
BYSL
CASP10
IFIH1
B
CHMP5
PNO1
CNPY3
CCDC22
LTV1
RIOK3
TBK1
IRF3
C20orf27
SF3B3
ACTR1B
TXNL4A
GNB2L1
RSL1D1
IL3
MXI1
GALNT7
VAMP5
LRGUK
SIL1
ZMAT3
LRRC8C
SEC11C
RNF130
SEL1L3
PAFAH2
SPTBN1
AZIN1
TRAPPC10
CHIC2
TMEM176B

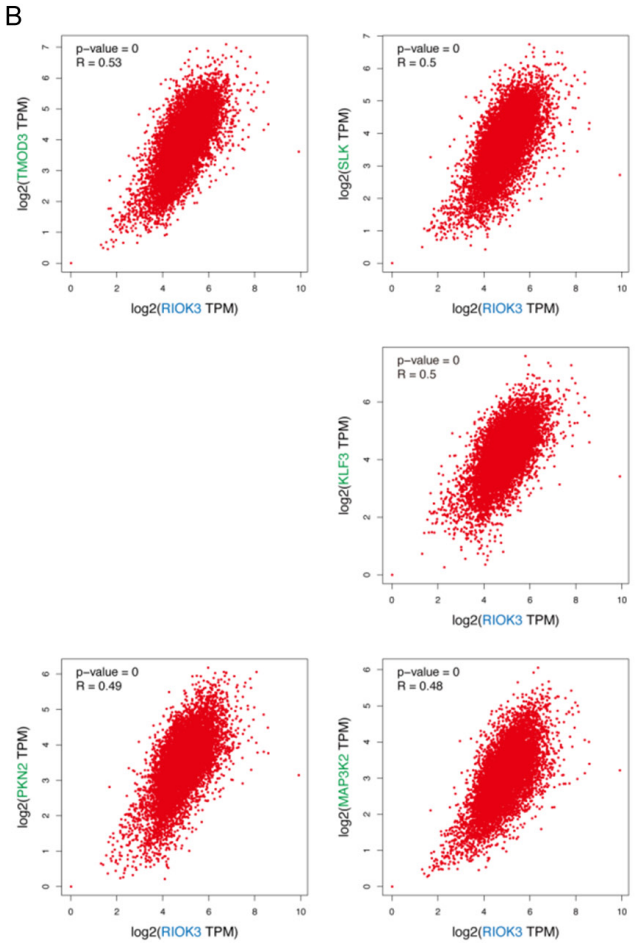
B
p−value = 0
R = 0.53
log2(TMOD3 TPM)
log2(RIOK3 TPM)
p−value = 0
R = 0.5
log2(SLK TPM)
log2(RIOK3 TPM)
p−value = 0
R = 0.5
log2(KLF3 TPM)
log2(RIOK3 TPM)
p−value = 0
R = 0.49
log2(PKN2 TPM)
log2(RIOK3 TPM)
p−value = 0
R = 0.48
log2(MAP3K2 TPM)
log2(RIOK3 TPM)

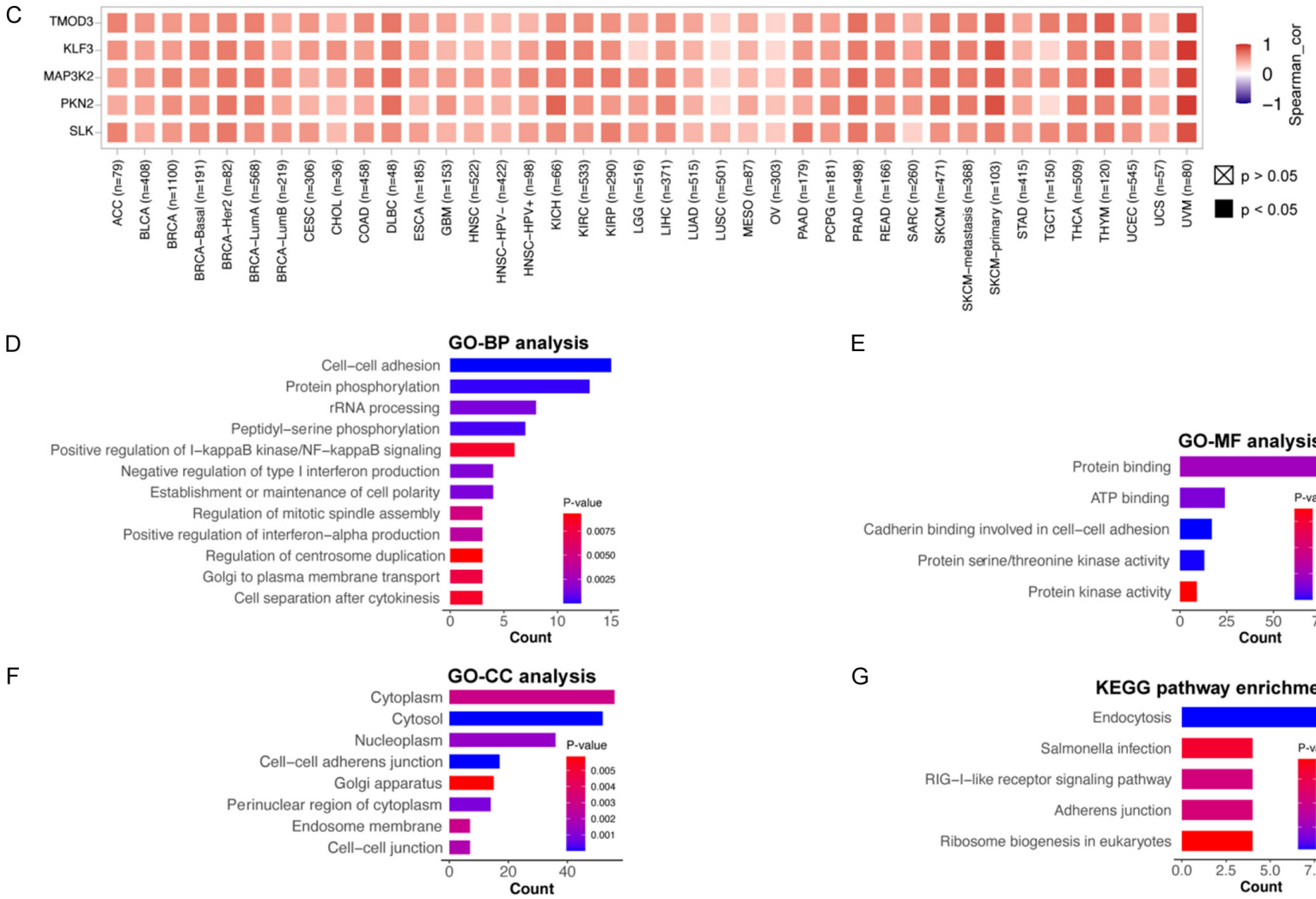

Figure 7. RIOK3-related gene enrichment and pathway analysis. (A) Protein-protein networks of RIOK3 (50 RIOK3-binding proteins supported by experimental evidence and text mining, based on the STRING database). (B) Expression correlation between RIOK3 and representative genes (TMOD3, SLK, KLF3, PKN2, and MAP3K2) of the top RIOK3-correlated genes in TCGA projects as determined by GEPIA2. (C) Heatmap of the expression correlation between RIOK3 and representative genes (TMOD3, SLK, KLF3, PKN2, and MAP3K2). (D-F) Functional enrichments are based on the RIOK3-binding proteins and RIOK3-correlated genes. GO (Gene ontology), GO-BP (Biological process) (D), GO-MF (Molecular function) (E), GO-CC (Cellular component) (F), KEGG (Kyoto encyclopedia of genes and genomes) (G).

PAAD, there is a stage-specific expression change of RIOK3. These findings show that RIOK3 could be used as a biomarker to predict the prognosis of cancer patients.

Gene mutations play an essential role in the etiology of several malignancies [35]. Amplification was the most common form of genetic alterations in TCGA tumor cases, especially in pancreatic adenocarcinoma and esophagogastric adenocarcinoma, according to our pan-cancer alteration analysis of RIOK3. Patients with RIOK3 mutations had a longer OS and PFS than those without the mutation. Under normal circumstances, the MMR system guarantees that DNA replication is stable. MLH1/PMS2, MSH2/MSH6, and EPCAM are heterodimers in the MMR system that can detect and fix gene alterations, such as base substitution, insertion, deletion, or mismatch during DNA replication [3]. Mutations or abnormalities in the MMR gene can accumulate genetic mistakes, leading to genomic or microsatellite instability and tumor formation [36]. In our research, RIOK3 was linked to TMB and MSI in various cancers, and it was linked to mutant MMR gene levels in almost all TCGA tumors, which could explain RIOK3's position in the MMR system, in which it mediates MMR's effects on TMB and MSI, encouraging the incidence and progression of malignancies.

In recent decades, the association between DNA methylation and cancer has increasingly been discovered [37, 38]. DNA methylation is a common type of epigenetic alteration of DNA that controls gene expression without changing the DNA sequence [39, 40]. By altering chromatin structure, DNA stability, and DNA conformation, DNA methylation normally decreases gene expression [41]. In malignant cells, hypermethylation within promoter regions frequently results in the silence or inactivation of tumor suppressor genes [42, 43]. DNA methylation of RIOK3 was downregulated in BLCA, BRCA, CESC, HNSC, KIRP, LUAD, LUSC, READ, THCA, and UCEC but increased in KIRC, according to the findings. There was a positive expression connection between RIOK3 and DNA methyltransferase in most TCGA tumors (21/33). Furthermore, there is a significant association between CECS, CHOL, DLBC, ESCA, KICH, KIRC, LIHC, LUSC, PAAD, STAD, TGCT, and UVM RIOK3 expression and methylation was identified. The methylation level of RIOK3 has been linked to cancer patient prognosis in some cases. For ESCA and KIRC, hypermethylation of RIOK3 indicates a bad prognosis, whereas it indicates a positive prognosis for LIHC. These findings suggest that methylation is a critical regulator of RIOK3 expression and may play a role in tumor growth. Unfortunately, there is no research on RIOK3 methylation, implying that the research in this field should be continued.

Emerging evidence has suggested that RIOK3 is related to innate immunity [31, 44-46], but the relationship between RIOK3 and tumor immune cell infiltration has not been elucidated. Evaluation using a variety of immune deconvolution methods, our data show that there is a statistically positive correlation between RIOK3 expression and neutrophil infiltration in COAD and KIRC tumors, a positive correlation between endothelial cells in KIRC and TGCT, and a negative correlation between cancer-associated fibroblasts in KIRC and STAD. The correlations between RIOK3 expression and TMB or MSI were also presented in this study. TMB and MSI have shown potential as predictive biomarkers with several applications, including associations reported between TMB and MSI levels and patient response to immune checkpoint inhibitor therapy in various cancers [36, 47]. Our data showed that RIOK3 expression was related to TMB (10/32) and MSI (10/32) indexes in about 1/3 of TCGA tumors and was associated with the expression of 47 common immune checkpoint genes, which further illustrated that RIOK3 might play an important role in tumor immunity. However, there is almost no report on the involvement of RIOK3 in tumor immunity. Therefore, the relationship between RIOK3 and tumor immunology is virgin land, a worthwhile study topic.

The last section investigated an extended version of RIOK3-binding proteins and the RIOK3 expression-correlated genes using GO terms and KEGG pathway enrichment analysis. The data described the possible molecular mechanism of RIOK3 in the process of tumorigenesis and development. RIOK3 is mainly involved in cell-cell adhesion, protein phosphorylation, innate immunity, mitosis, establishment and maintenance of cell polarity, and other important biological processes in tumor cells, and these results are almost consistent with previous reports [15-17, 31, 33, 44, 46].

In conclusion, statistical associations between RIOK3 expression and clinical prognosis, DNA methylation, immune cell infiltration, tumor mutation burden, and microsatellite instability in a variety of human tumors were discovered as a result of our comprehensive pan-cancer analysis of RIOK3, helping to clarify the molecular mechanism of RIOK3 in tumorigenesis from a variety of perspectives.

Acknowledgements

This study was supported by the Science and Technology Program foundation of Henan Province, China (No. 192102310097), Nature Science Foundation of Henan Province, China (No. 212300410381), and Key Scientific Research Projects of Higher Education Institutions in Henan Province, China (No. 19A320005).

Disclosure of conflict of interest

None.

Address correspondence to: Feng Ren and Jinghang Zhang, Department of Pathology, The First Affiliated Hospital of Xinxiang Medical University, No. 88 WH Jiankang Road, Xinxiang 453003, Henan, China. Tel: +86-0373-3029116; Fax: +86-0373-3029116; E-mail: 1215377283@qq.com (FR); Tel: +86-0373-4404227; Fax: +86-0373-4404227; E-mail: zhangjinghang1116@163.com (JHZ)

References

[1] ICGC/TCGA Pan-Cancer Analysis of Whole Genomes Consortium. Pan-cancer analysis of whole genomes. Nature 2020; 578: 82-93.

[2] Pleasance ED, Cheetham RK, Stephens PJ, McBride DJ, Humphray SJ, Greenman CD, Varela I, Lin ML, Ordonez GR, Bignell GR, Ye K, Alipaz J, Bauer MJ, Beare D, Butler A, Carter RJ, Chen L, Cox AJ, Edkins S, Kokko-Gonzales PI, Gormley NA, Grocock RJ, Haudenschild CD, Hims MM, James T, Jia M, Kingsbury Z, Leroy C, Marshall J, Menzies A, Mudie LJ, Ning Z, Royce T, Schulz-Trieglaff OB, Spiridou A, Stebbings LA, Szajkowski L, Teague J, Williamson D, Chin L, Ross MT, Campbell PJ, Bentley DR, Futreal PA and Stratton MR. A comprehensive catalogue of somatic mutations from a human cancer genome. Nature 2010; 463: 191-196.

[3] Antoniotti C, Korn WM, Marmorino F, Rossini D, Lonardi S, Masi G, Randon G, Conca V, Boccaccino A, Tomasello G, Passardi A, Swensen J, Ugolini C, Oberley M, Tamburini E, Casagrande M, Domenyuk V, Fontanini G, Giordano M, Abraham J, Spetzler D, Falcone A, Lenz HJ and Cremolini C. Tumor mutational burden, microsatellite instability, and actionable alterations in metastatic colorectal cancer: next-generation sequencing results of TRIBE2 study. Eur J Cancer 2021; 155: 73-84.

[4] Armendariz-Castillo I, Lopez-Cortes A, Garcia-Cardenas J, Guevara-Ramirez P, Leone PE, Perez-Villa A, Yumiceba V, Zambrano AK, Guerrero S and Paz-Y-Miño C. TCGA pan-cancer genomic analysis of alternative lengthening of telomeres (ALT) related genes. Genes (Basel) 2020; 11: 834.

[5] Cancer Genome Atlas Research Network; Weinstein JN, Collisson EA, Mills GB, Shaw KR, Ozenberger BA, Ellrott K, Shmulevich I, Sander C and Stuart JM. The cancer genome atlas pan-cancer analysis project. Nat Genet 2013; 45: 1113-1120.

[6] Blum A, Wang P and Zenklusen JC. SnapShot: TCGA-analyzed tumors. Cell 2018; 173: 530.

[7] Clough E and Barrett T. The gene expression omnibus database. Methods Mol Biol 2016; 1418: 93-110.

[8] Tomczak K, Czerwinska P and Wiznerowicz M. The cancer genome atlas (TCGA): an immeasurable source of knowledge. Contemp Oncol (Pozn) 2015; 19: A68-77.

[9] Zheng Y, Huang G, Silva TC, Yang Q, Jiang YY, Koeffler HP, Lin DC and Berman BP. A pan-cancer analysis of CpG Island gene regulation reveals extensive plasticity within polycomb target genes. Nat Commun 2021; 12: 2485.

[10] Napoli M, Li X, Ackerman HD, Deshpande AA, Barannikov I, Pisegna MA, Bedrosian I, Mitsch J, Quinlan P, Thompson A, Rajapakshe K, Coarfa C, Gunaratne PH, Marchion DC, Magliocco AM, Tsai KY and Flores ER. Pan-cancer analysis reveals TAp63-regulated oncogenic lncRNAs that promote cancer progression through AKT activation. Nat Commun 2020; 11: 5156.

[11] Ghoshdastider U, Rohatgi N, Mojtabavi Naeini M, Baruah P, Revkov E, Guo YA, Rizzetto S, Wong AML, Solai S, Nguyen TT, Yeong JPS, Iqbal J, Tan PH, Chowbay B, Dasgupta R and Skanderup AJ. Pan-cancer analysis of ligand-receptor cross-talk in the tumor microenvironment. Cancer Res 2021; 81: 1802-1812.

[12] LaRonde-LeBlanc N and Wlodawer A. The RIO kinases: an atypical protein kinase family required for ribosome biogenesis and cell cycle progression. Biochim Biophys Acta 2005; 1754: 14-24.

[13] Baumas K, Soudet J, Caizergues-Ferrer M, Faubladier M, Henry Y and Mougin A. Human RioK3 is a novel component of cytoplasmic

pre-40S pre-ribosomal particles. RNA Biol 2012; 9: 162-174.
[14] Henras AK, Plisson-Chastang C, O'Donohue MF, Chakraborty A and Gleizes PE. An overview of pre-ribosomal RNA processing in eukaryotes. Wiley Interdiscip Rev RNA 2015; 6: 225-242.
[15] Singleton DC, Rouhi P, Zois CE, Haider S, Li JL, Kessler BM, Cao Y and Harris AL. Hypoxic regulation of RIOK3 is a major mechanism for cancer cell invasion and metastasis. Oncogene 2015; 34: 4713-4722.
[16] Kimmelman AC, Hezel AF, Aguirre AJ, Zheng H, Paik JH, Ying H, Chu GC, Zhang JX, Sahin E, Yeo G, Ponugoti A, Nabioullin R, Deroo S, Yang S, Wang X, McGrath JP, Protopopova M, Ivanova E, Zhang J, Feng B, Tsao MS, Redston M, Protopopov A, Xiao Y, Futreal PA, Hahn WC, Klimstra DS, Chin L and DePinho RA. Genomic alterations link Rho family of GTPases to the highly invasive phenotype of pancreas cancer. Proc Natl Acad Sci U S A 2008; 105: 19372-19377.
[17] Zhang T, Ji D, Wang P, Liang D, Jin L, Shi H, Liu X, Meng Q, Yu R and Gao S. The atypical protein kinase RIOK3 contributes to glioma cell proliferation/survival, migration/invasion and the AKT/mTOR signaling pathway. Cancer Lett 2018; 415: 151-163.
[18] Giri U, Ashorn CL, Ramdas L, Stivers DN, Coombes K, El-Naggar AK, Ang KK and Story MD. Molecular signatures associated with clinical outcome in patients with high-risk head-and-neck squamous cell carcinoma treated by surgery and radiation. Int J Radiat Oncol Biol Phys 2006; 64: 670-677.
[19] Roesch A, Vogt T, Stolz W, Dugas M, Landthaler M and Becker B. Discrimination between gene expression patterns in the invasive margin and the tumor core of malignant melanomas. Melanoma Res 2003; 13: 503-509.
[20] Huo G, Wang Y, Chen J, Song Y, Zhang C, Guo H, Zuo R, Zhu F, Cui J, Chen W, Chen W and Chen P. A pan-cancer analysis of the oncogenic role of twinfilin actin binding protein 1 in human tumors. Front Oncol 2021; 11: 692136.
[21] Tang Z, Kang B, Li C, Chen T and Zhang Z. GEPIA2: an enhanced web server for large-scale expression profiling and interactive analysis. Nucleic Acids Res 2019; 47: W556-W560.
[22] Chandrashekar DS, Bashel B, Balasubramanya SAH, Creighton CJ, Ponce-Rodriguez I, Chakravarthi B and Varambally S. UALCAN: a portal for facilitating tumor subgroup gene expression and survival analyses. Neoplasia 2017; 19: 649-658.
[23] Hou GX, Liu P, Yang J and Wen S. Mining expression and prognosis of topoisomerase isoforms in non-small-cell lung cancer by using oncomine and Kaplan-Meier plotter. PLoS One 2017; 12: e0174515.
[24] Gao J, Aksoy BA, Dogrusoz U, Dresdner G, Gross B, Sumer SO, Sun Y, Jacobsen A, Sinha R, Larsson E, Cerami E, Sander C and Schultz N. Integrative analysis of complex cancer genomics and clinical profiles using the cBioPortal. Sci Signal 2013; 6: pl1.
[25] Wu P, Heins ZJ, Muller JT, Katsnelson L, de Bruijn I, Abeshouse AA, Schultz N, Fenyo D and Gao J. Integration and analysis of CPTAC proteomics data in the context of cancer genomics in the cBioPortal. Mol Cell Proteomics 2019; 18: 1893-1898.
[26] Li Y, Ge D and Lu C. The SMART App: an interactive web application for comprehensive DNA methylation analysis and visualization. Epigenetics Chromatin 2019; 12: 71.
[27] Ding W, Chen G and Shi T. Integrative analysis identifies potential DNA methylation biomarkers for pan-cancer diagnosis and prognosis. Epigenetics 2019; 14: 67-80.
[28] Li T, Fu J, Zeng Z, Cohen D, Li J, Chen Q, Li B and Liu XS. TIMER2.0 for analysis of tumor-infiltrating immune cells. Nucleic Acids Res 2020; 48: W509-W514.
[29] Szklarczyk D, Gable AL, Lyon D, Junge A, Wyder S, Huerta-Cepas J, Simonovic M, Doncheva NT, Morris JH, Bork P, Jensen LJ and Mering CV. STRING v11: protein-protein association networks with increased coverage, supporting functional discovery in genome-wide experimental datasets. Nucleic Acids Res 2019; 47: D607-D613.
[30] Jiao X, Sherman BT, Huang da W, Stephens R, Baseler MW, Lane HC and Lempicki RA. DAVID-WS: a stateful web service to facilitate gene/protein list analysis. Bioinformatics 2012; 28: 1805-1806.
[31] Feng J, De Jesus PD, Su V, Han S, Gong D, Wu NC, Tian Y, Li X, Wu TT, Chanda SK and Sun R. RIOK3 is an adaptor protein required for IRF3-mediated antiviral type I interferon production. J Virol 2014; 88: 7987-7997.
[32] Zhang L, Flygare J, Wong P, Lim B and Lodish HF. miR-191 regulates mouse erythroblast enucleation by down-regulating Riok3 and Mxi1. Genes Dev 2011; 25: 119-124.
[33] Shan J, Wang P, Zhou J, Wu D, Shi H and Huo K. RIOK3 interacts with caspase-10 and negatively regulates the NF-kappaB signaling pathway. Mol Cell Biochem 2009; 332: 113-120.
[34] Tariki M, Wieczorek SA, Schneider P, Banfer S, Veitinger S, Jacob R, Fendrich V and Lauth M. RIO kinase 3 acts as a SUFU-dependent positive regulator of hedgehog signaling. Cell Signal 2013; 25: 2668-2675.
[35] Martinez-Jimenez F, Muinos F, Sentis I, Deu-Pons J, Reyes-Salazar I, Arnedo-Pac C, Mularo-

ni L, Pich O, Bonet J, Kranas H, Gonzalez-Perez A and Lopez-Bigas N. A compendium of mutational cancer driver genes. Nat Rev Cancer 2020; 20: 555-572.
[36] Rizzo A, Ricci AD and Brandi G. PD-L1, TMB, MSI, and other predictors of response to immune checkpoint inhibitors in biliary tract cancer. Cancers (Basel) 2021; 13: 558.
[37] Gu T and Goodell MA. The push and pull of DNA methylation. Science 2021; 372: 128-129.
[38] Feinberg A. DNA methylation in cancer: three decades of discovery. Genome Med 2014; 6: 36.
[39] Schubeler D. Function and information content of DNA methylation. Nature 2015; 517: 321-326.
[40] Licht JD. DNA methylation inhibitors in cancer therapy: the immunity dimension. Cell 2015; 162: 938-939.
[41] Luo C, Hajkova P and Ecker JR. Dynamic DNA methylation: in the right place at the right time. Science 2018; 361: 1336-1340.
[42] Daura-Oller E, Cabre M, Montero MA, Paternain JL and Romeu A. Specific gene hypomethylation and cancer: new insights into coding region feature trends. Bioinformation 2009; 3: 340-343.
[43] Wang YP and Lei QY. Metabolic recoding of epigenetics in cancer. Cancer Commun (Lond) 2018; 38: 25.
[44] Takashima K, Oshiumi H, Takaki H, Matsumoto M and Seya T. RIOK3-mediated phosphorylation of MDA5 interferes with its assembly and attenuates the innate immune response. Cell Rep 2015; 11: 192-200.
[45] Gokhale NS, McIntyre ABR, Mattocks MD, Holley CL, Lazear HM, Mason CE and Horner SM. Altered m(6)A modification of specific cellular transcripts affects flaviviridae infection. Mol Cell 2020; 77: 542-555.
[46] Shen Y, Tang K, Chen D, Hong M, Sun F, Wang S, Ke Y, Wu T, Sun R, Qian J and Du Y. Riok3 inhibits the antiviral immune response by facilitating TRIM40-mediated RIG-I and MDA5 degradation. Cell Rep 2021; 35: 109272.
[47] Kim JY, Kronbichler A, Eisenhut M, Hong SH, van der Vliet HJ, Kang J, Shin JI and Gamerith G. Tumor mutational burden and efficacy of immune checkpoint inhibitors: a systematic review and meta-analysis. Cancers (Basel) 2019; 11: 1798.

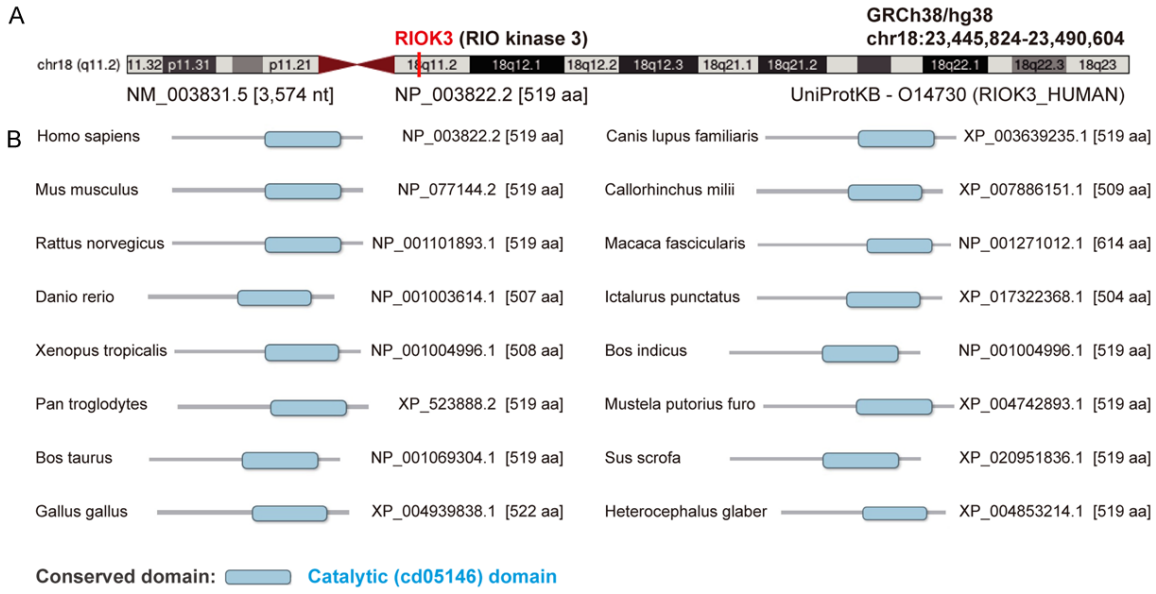

Figure S1. Structural characteristics of RIOK3 in different species. A. Human RIOK3 gene location in hg38. B. Conserved protein domains of RIOK3 across different species.

Figure S2. Expression levels of RIOK3 in different cells and tissues under normal physiological conditions. A. Expression levels of RIOK3 in different tissues based on HPA, GTEx, and FANTOM5 database. B. Expression levels of RIOK3 in different blood cell types based on the HPA, Monaco, and Schmiedel datasets.

A **Gastric cancer**

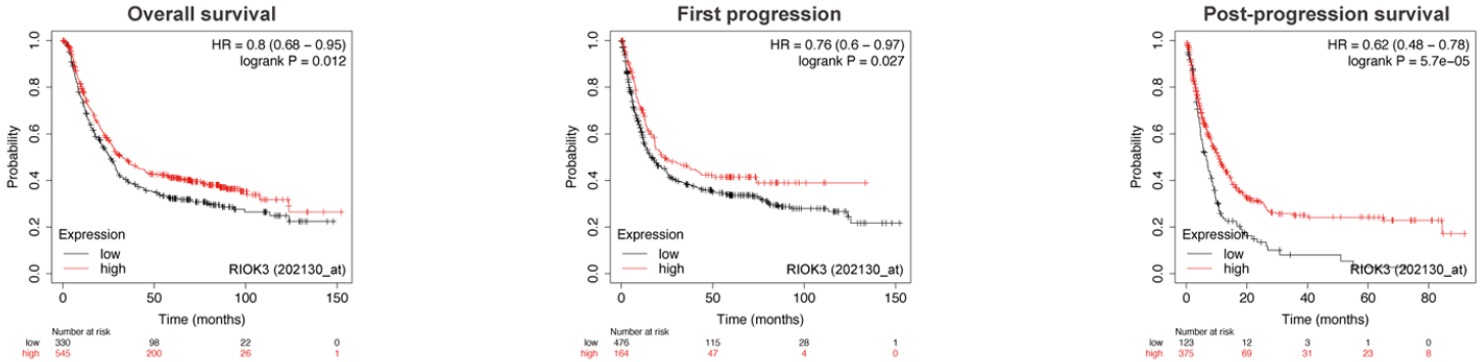

B **Lung cancer**

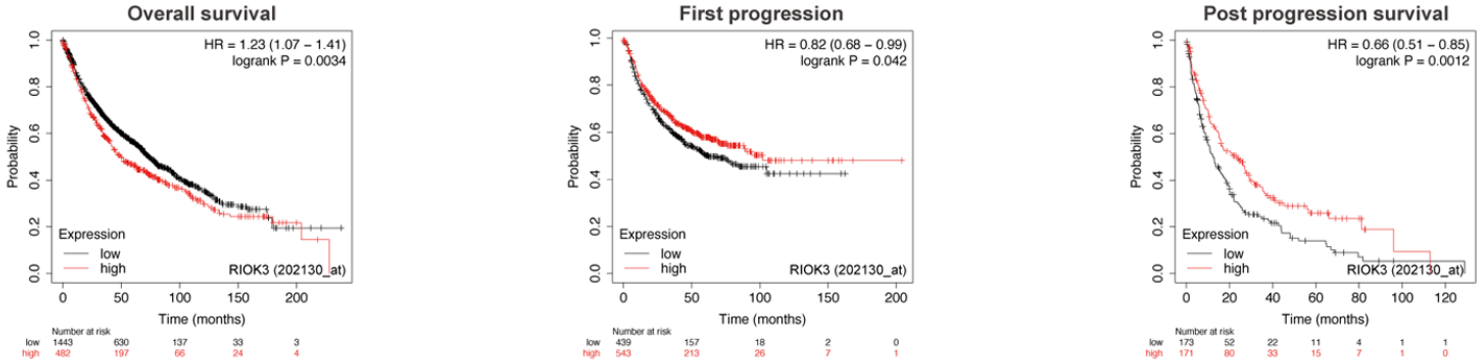

C **Ovarian cancer**

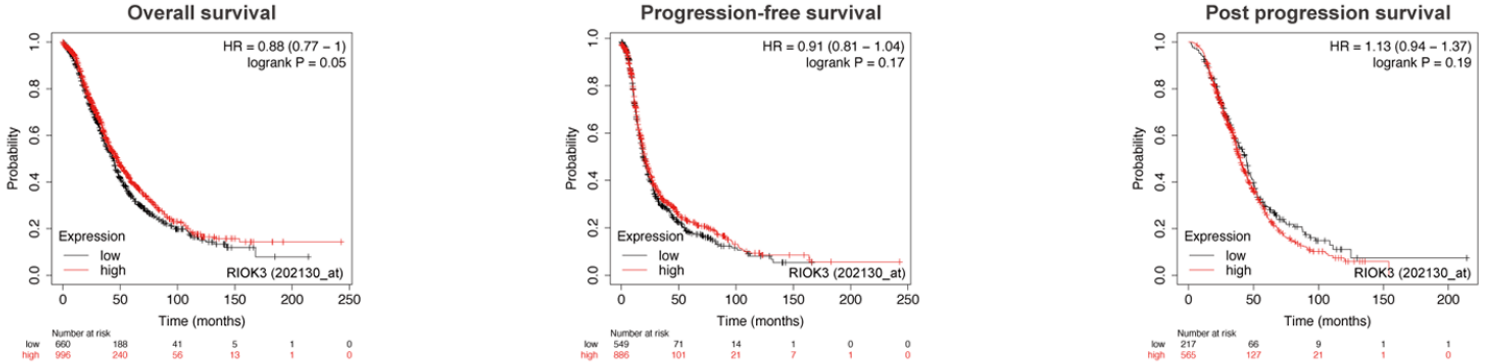

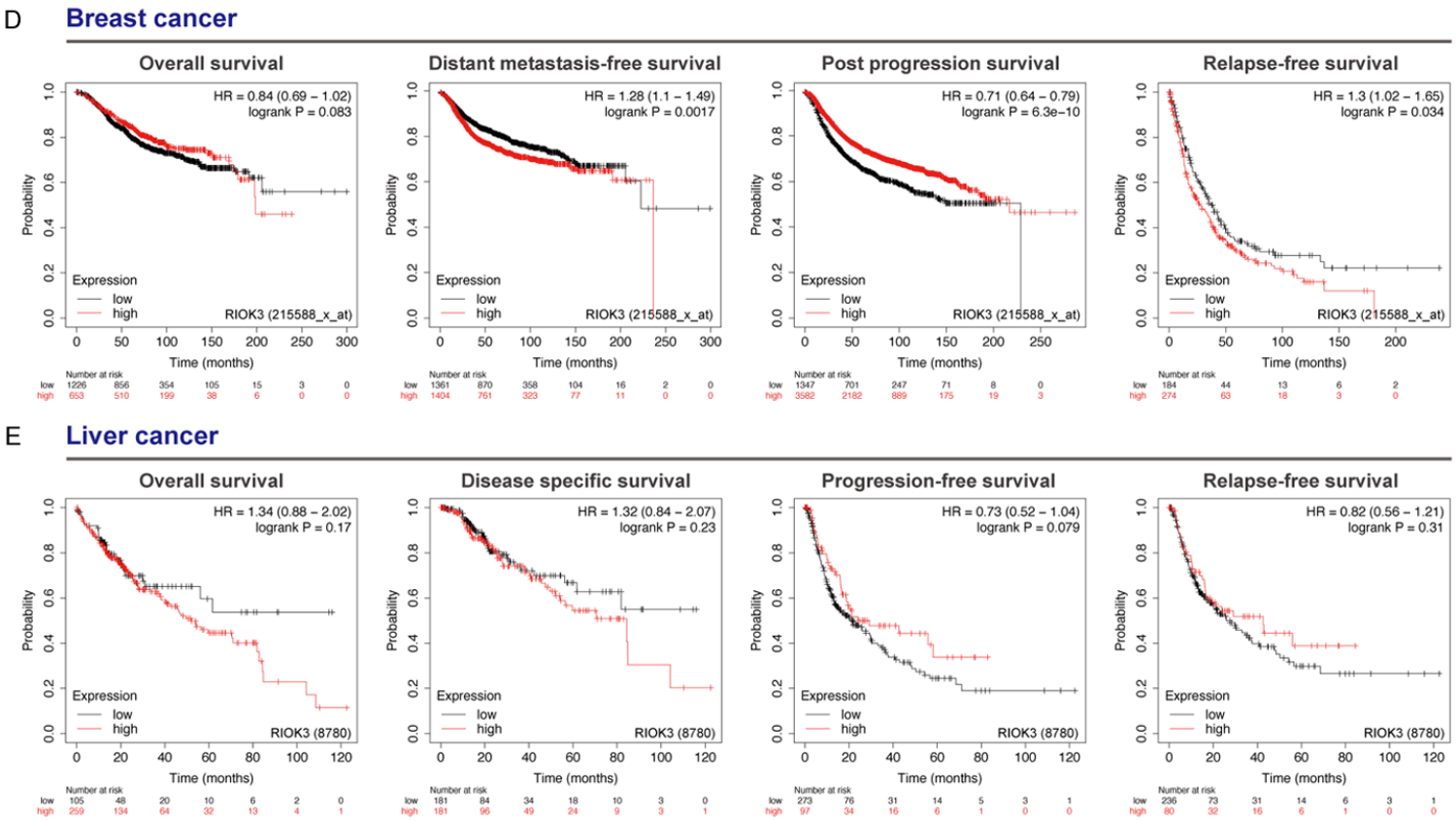

Figure S3. Relationship between RIOK3 expression levels and prognosis in different cancer patients. Kaplan-Meier plotter was used to perform the survival analyses in gastric cancer (A), lung cancer (B), ovarian cancer (C), breast cancer (D), and liver cancer (E) patients.

Pan-cancer analysis of RIO kinase 3

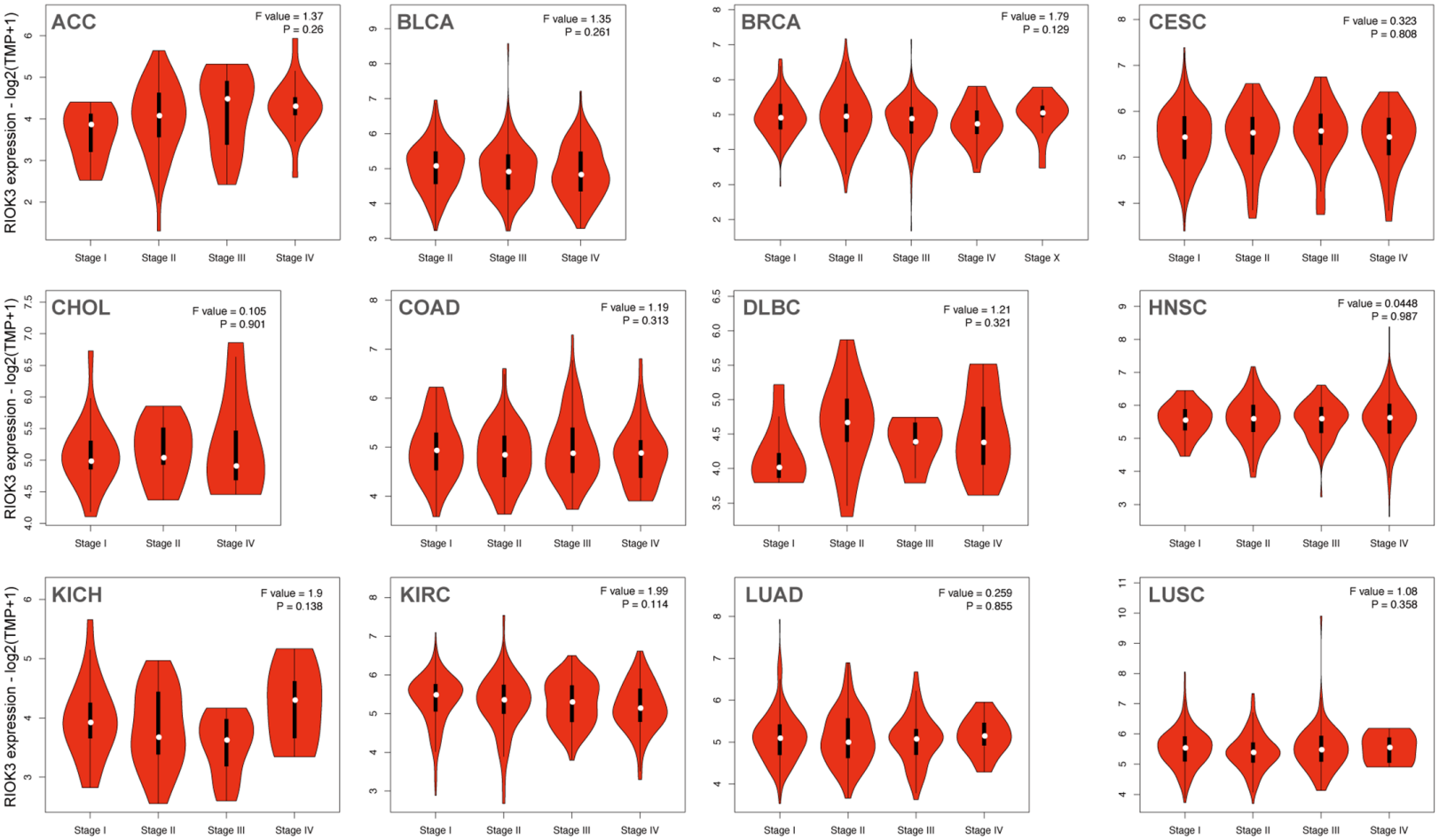

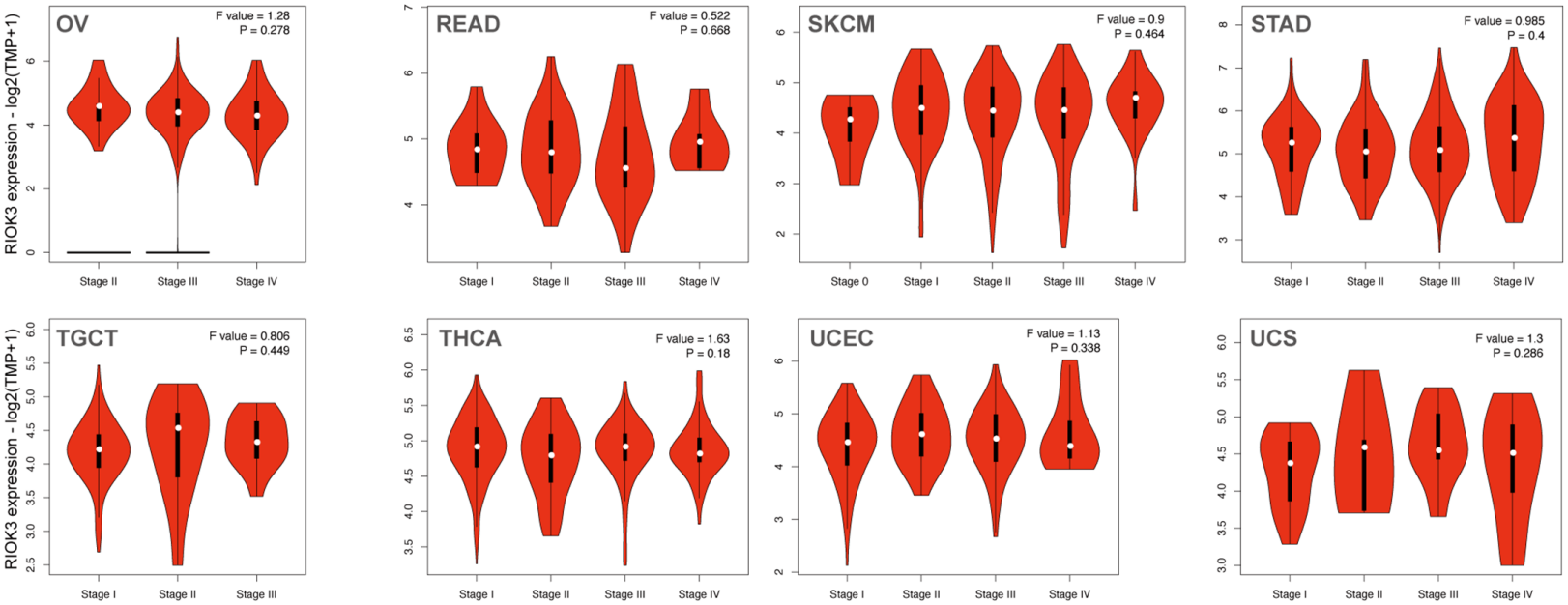

Figure S4. The stage-dependent expression level of RIOK3. Pathological stage plot derived for RIOK3 expression data in GEPIA2 for ACC, BLCA, BRCA, CESC, CHOL, COAD, DLBC, HNSC, KICH, KIRC, LUAD, LUSC, OV, READ, SKCM, STAD, TGCT, THCA, UCEC, and UCS. These data are statistically non-significant.

A

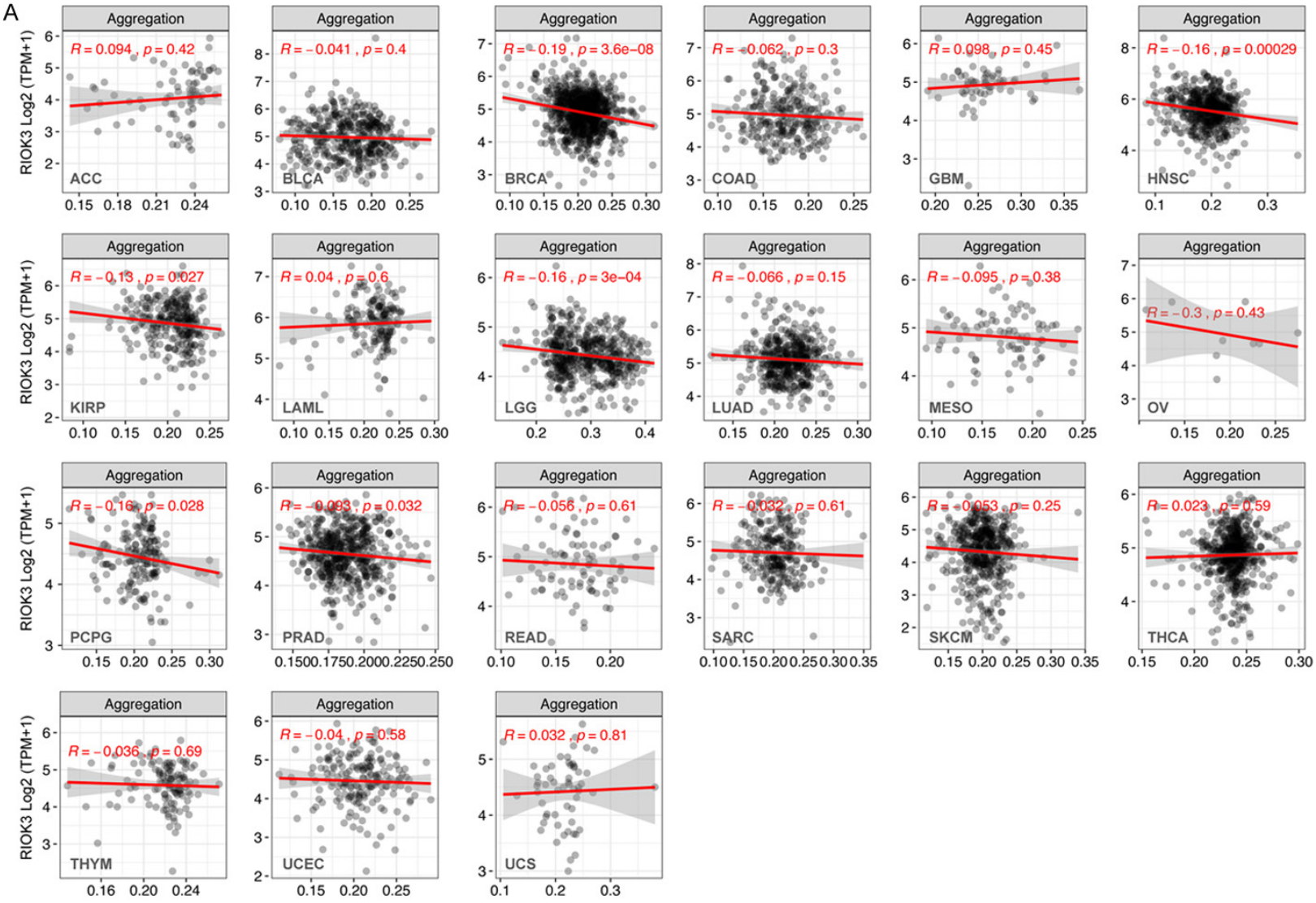
Aggregation
RIOK3 Log2 (TPM+1)
R = 0.094 , p = 0.42
ACC
R = −0.041 , p = 0.4
BLCA
R = −0.19 , p = 3.6e−08
BRCA
R = −0.062 , p = 0.3
COAD
R = 0.098 , p = 0.45
GBM
R = −0.16 , p = 0.00029
HNSC
R = −0.13 , p = 0.027
KIRP
R = 0.04 , p = 0.6
LAML
R = −0.16 , p = 3e−04
LGG
R = −0.066 , p = 0.15
LUAD
R = −0.095 , p = 0.38
MESO
R = −0.3 , p = 0.43
OV
R = −0.16 , p = 0.028
PCPG
R = −0.093 , p = 0.032
PRAD
R = −0.056 , p = 0.61
READ
R = −0.032 , p = 0.61
SARC
R = −0.053 , p = 0.25
SKCM
R = 0.023 , p = 0.59
THCA
R = −0.036 , p = 0.69
THYM
R = −0.04 , p = 0.58
UCEC
R = 0.032 , p = 0.81
UCS

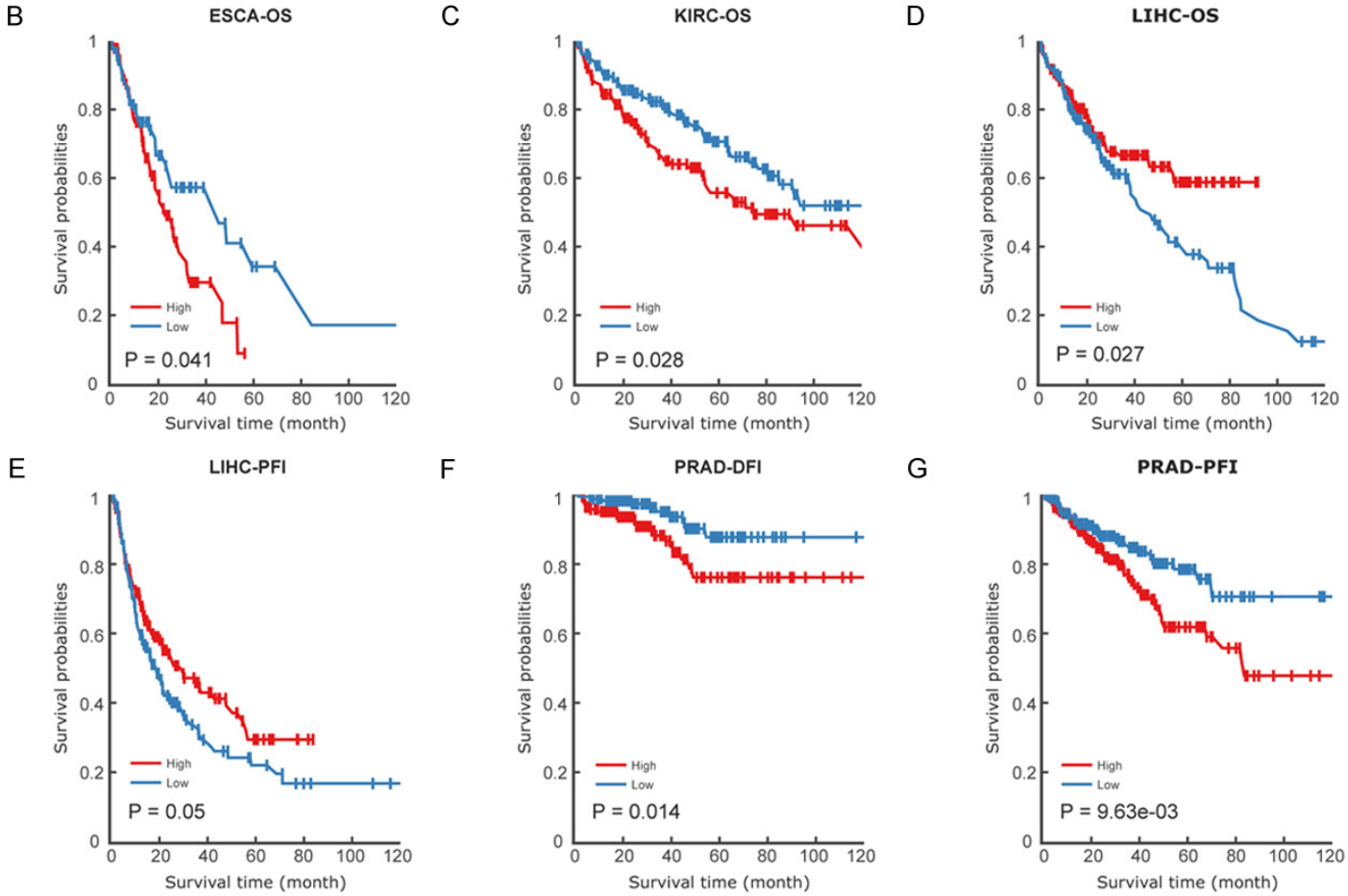

Figure S5. Analysis of RIOK3 DNA methylation data in TCGA. A. Correlation between gene expression and methylation value (beta-value) of RIOK3 in different tumors of TCGA. These data are statistically non-significant (R < 0.2 or P > 0.05). B-G. Relationship between CpG-aggregated methylation value of RIOK3 and prognosis in different cancer patients. DNMIVD tool was used to perform the survival analyses (OS, PFI, and DFI) in ESCA, KIRC, LIHC, and PRAD patients in the TCGA project. Only statistically significant data are shown here.

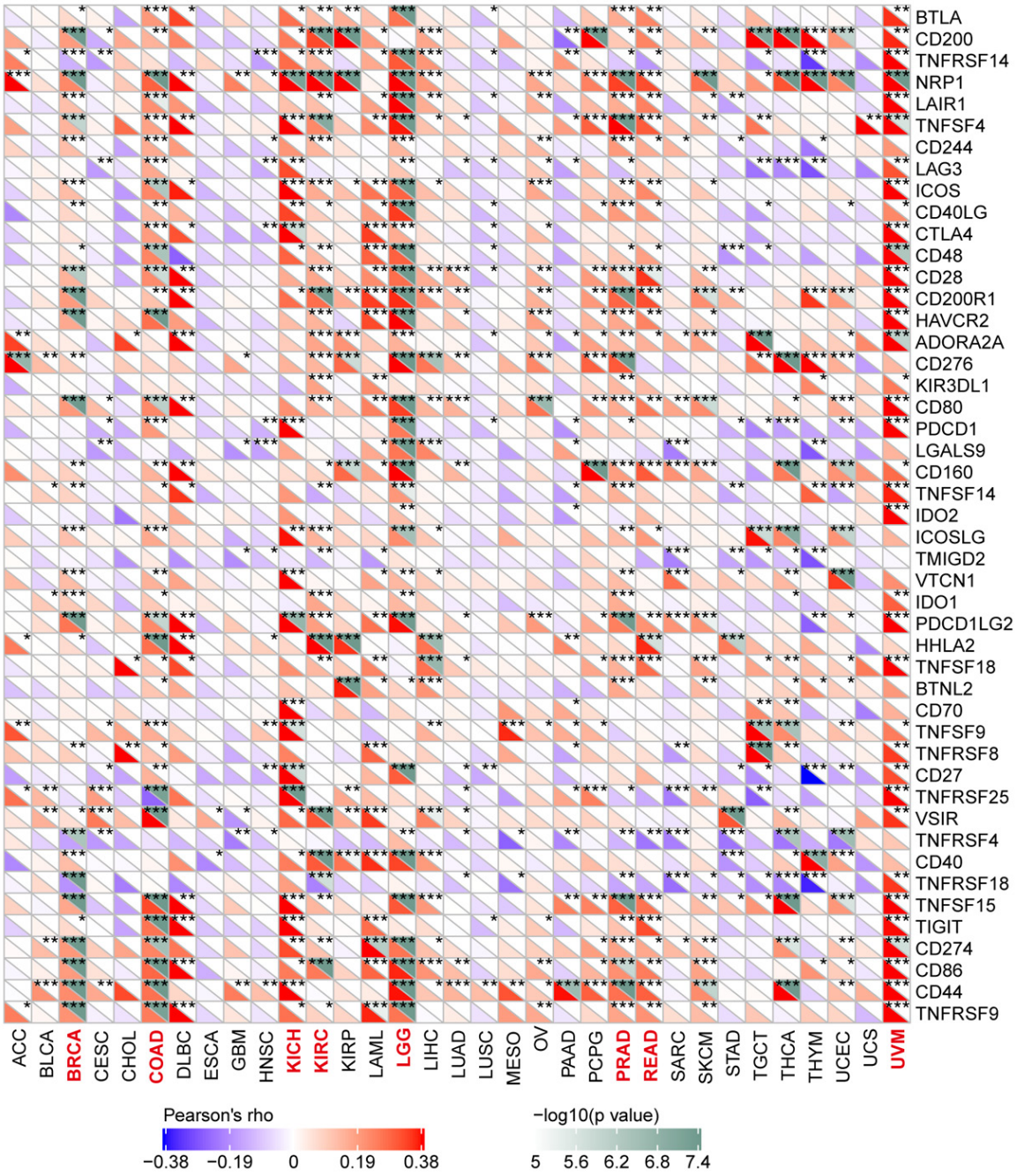

Figure S6. Correlation analysis of RIOK3 expression with 47 common immune checkpoint genes in TCGA tumors.

Table S1. Kaplan-Meier survival analysis of RIOK3 methylation value

Disease	OS	DFI	PFI
BLCA	0.5881	0.3338	0.2956
BRCA	0.8536	0.7583	0.9708
CESC	0.9678	0.1176	0.7615
CHOL	0.5664	0.4276	0.4386
COAD	0.6227	0.0615	0.3896
ESCA	0.0412*	0.8500	0.0905
GBM	0.4167	Nan	0.6436
HNSC	0.2372	0.9201	0.1273
KIRC	0.0279*	0.4201	0.0736
KIRP	0.4674	0.1335	0.0925
LIHC	0.0268*	0.0799	0.0497*
LUAD	0.8794	0.6841	0.8018
LUSC	0.1034	0.5266	0.0950
PAAD	0.6647	0.3129	0.5540
PCPG	0.1812	0.9506	0.4085
PRAD	0.2177	0.0143*	0.0096**
READ	0.8081	0.1826	0.6706
SARC	0.9225	0.3552	0.5869
SKCM	0.0628	1.0000	0.0996
STAD	0.7675	0.9094	0.2227
THCA	0.0528	0.3454	0.5904
THYM	0.9682	1.0000	0.7004

Using median DNA methylation beta values as threshold to divide samples into High and Low group. OS: Overall Survival time; DFI: Disease-free Interval; PFI: Progression-free Interval. *$P < 0.05$, **$P < 0.01$, Na: not a number.